Original paper

# The inner architecture of tourmaline crystals, as inferred from the morphology of color zones in thin slices

## Paul RUSTEMEYER

*Waldackerweg 7, 79194 Gundelfingen, Germany; rustemeyer-gundelfingen@t-online.de*

Tourmaline crystals are known for their variety of morphologies, intricate and complex growth features, and wide spectrum of colors. If dark tourmalines crystals are sliced and ground to an optimum thickness, intensely colored intrasectoral zones and other fine features become visible. Evaluating a series of slices lead to an understanding of the three-dimensional inner morphology of the crystal.

A screening of thousands of dark tourmaline crystals led to a collection of more than 30 000 slices, from which the most important morphological features are revealed. These features include sector zones, intrasectoral color zones, concentric growth-zones, diverse types of delta-shaped features as second intrasectoral triangular color domains, various mechanisms of repair of fracture surfaces (healing) and of corroded crystals. Six mechanisms are documented in subdivision phenomena, in which a single crystal is subdivided into a bundle of parallel needle-shaped crystals.

Hollow skeletal crystals and monocrystalline dendritic growth were found in the core of freely crystallized parallel aggregates. Such parallel aggregates with normal compact crystals in the same pocket could support the hypothesis that crystallization occurred from coexisting media, a melt and an aqueous phase that had undergone phase separation. In addition, structures similar to the parallel aggregates were found in graphic intergrowths of tourmaline with quartz, feldspar or mica.

## 1. Introduction

The inner architecture of tourmaline crystals, made visible by slicing, was first reported in multicolored tourmaline crystals found in the Anjanabonoina pegmatite (Lacroix 1908). The striking zonation of the multicolored slices of fluor-liddicoatite was subsequently illustrated by Benesch (1985), Rustemeyer (2003, 2011) and Peetsch (2011). Some black crystals of tourmaline also become colored if examined in thin sections, but many of these outwardly black crystals remain black at a thickness of 30 μm. Only if they are further thinned to a thickness of 20 to 10 μm do they display colors, and they also may contain an enormous variety of unexpected textures. In 1994, this "discovery" was the starting point of an intense screening of the inner architecture of thousands of "black" tourmaline crystals. Fantastic new worlds were revealed, with phenomena never before documented (Rustemeyer 2003b, 2011, 2015a, 2018, 2022). Crystals of dark tourmaline commonly record variations in their growth medium with changes of color and shape. Such crystals are ideal for studying growth phenomena, even in the absence of analytical measurements, as the color zones clearly make their inner morphology visible.

Three lines of action were combined to document the zonation patterns in black tourmaline crystals. Firstly, the thickness of the slices was defined by the optimum saturation of colors. It varies between 1 mm and 10 μm. Such optimum saturation is achieved when details emerge in the dark areas of the slice, while the details in the light areas are still visible (Fig. 1a). Secondly, a series of slices through the crystal captures the entire internal three-dimensional array of microtextures in the sliced part of the crystal (Fig. 1b). Furthermore, a perspective view of a stack of slices can make the evolution of zones within the crystal easy to comprehend (Fig. 1c). Thirdly, processing several crystals from the same location, even from the same pocket, commonly shows an interesting variety of structures.

Most of the slices were cut perpendicular to the *c* axis, called "crosscuts". Cuts along the *c* axis also reveal growth-induced zonation; because of strong dichroism. However, these are predominantly brown in color. Thus, slices along the *c* axis ("longitudinal cuts") display a lower density of color and are less attractive. In addition, at an optimum setting of color saturation, they are thicker; as a result, microscopic details generally overlap and appear less sharp. In summary, crosscuts possess a higher depth of color and a more intense coloration; they display more sharply defined features and are thinner. Figure 1d gives an impression of the sharpness in a segment 2 mm wide.

The author's screening of thousands of tourmaline crystals has led to a collection of more than 30,000 slices.
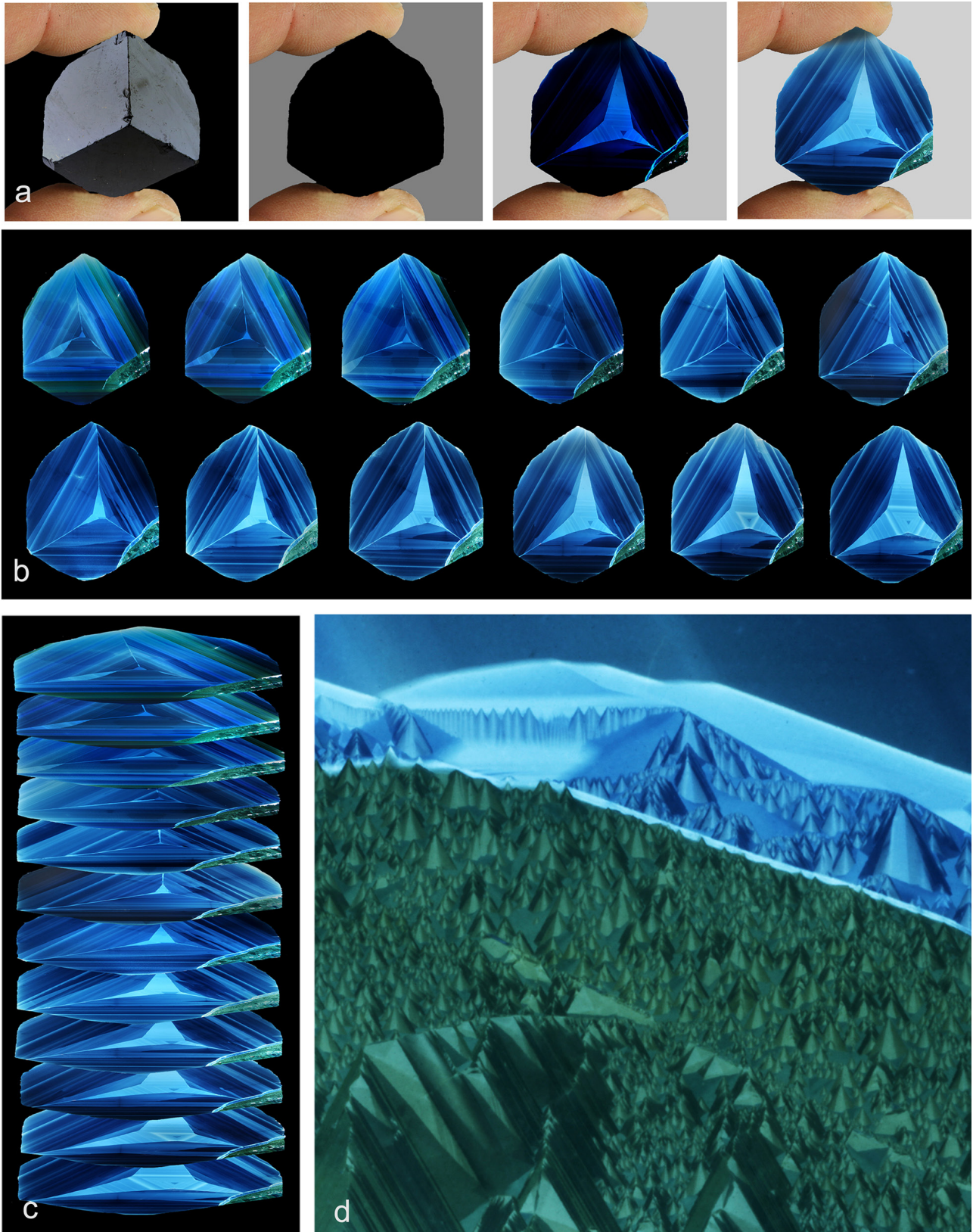
**Fig. 1** A tourmaline crystal is processed from a thick section to a thin section. Sample from Minas Gerais, Ø (diameter) 32 mm. **a** – step by step processing. These slices reveals sector zoning, intrasectoral color zones and a green area indicating the presence of a fracture and subsequent healing of the scar; **b** – series of slices prepared from the crystal; **c** – view on a stack of slices; **d** – detailed illustration of the green zone, the site of healing, 2 mm wide.
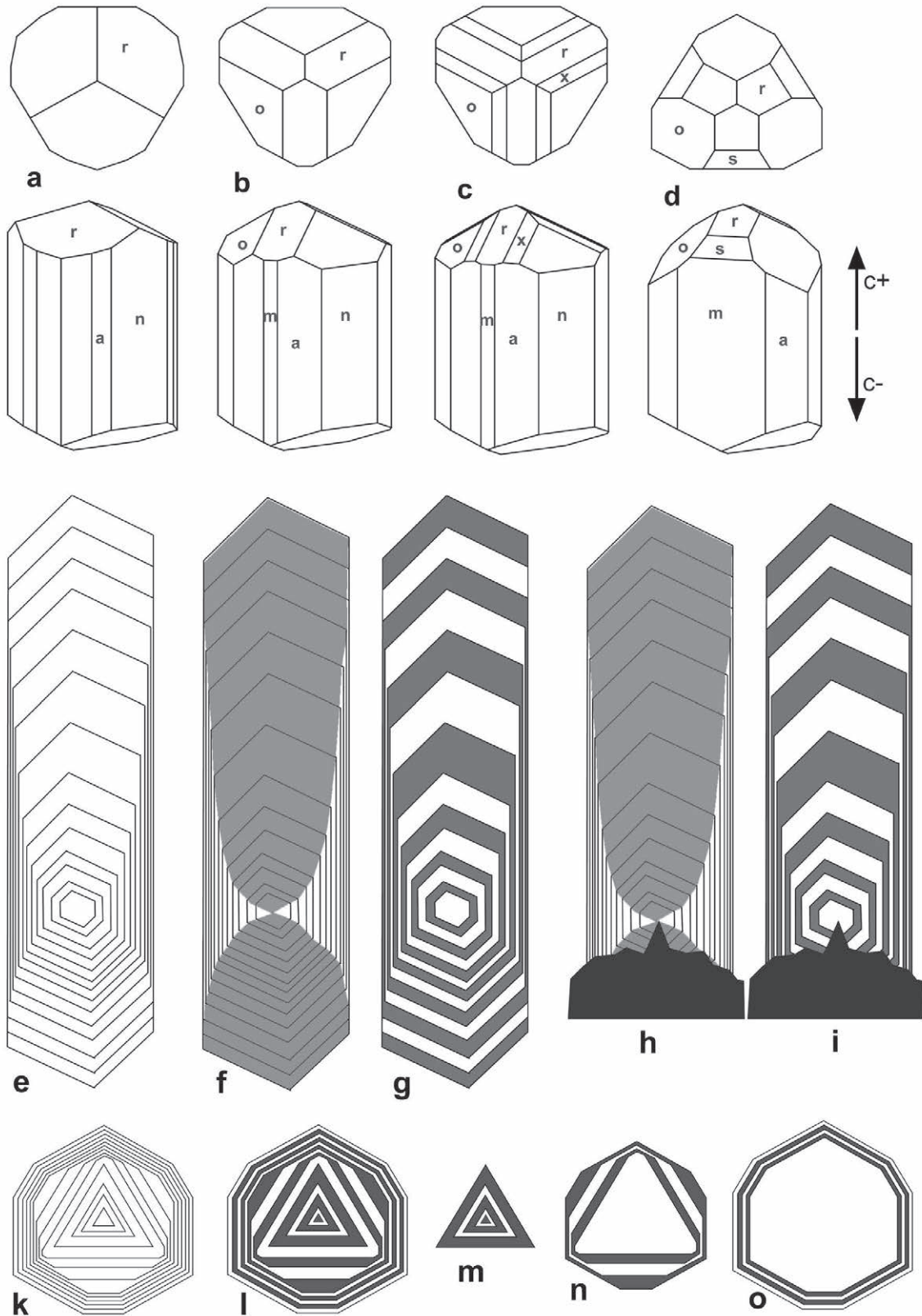
**Fig. 2a–d:** Some examples of typical tourmaline shapes; **e–o:** Boundaries of color zones, sector zones and concentric growth zones in longitudinal and crosscuts of a doubly or singly terminated tourmaline (combination of trigonal pyramid, hexagonal and trigonal prism). e, k: boundaries of color zones, f, h: sector zones of the **r** and **–r** forms, g, i, l: and concentric growth zones in longitudinal and cross cuts of a double or single terminated tourmaline (combination of trigonal pyramid **r**, hexagonal and trigonal prism).

So far, findings have been published in German articles. (e.g., Rustemeyer 2003b, 2011, 2015a, 2019a,b, 2022, Rustemeyer and Müller 2017, Rustemeyer and Prögler 2019). This was the basis for preparing this review paper illustrating the more common zonation patterns in dark tourmaline crystals.

## 2. Sector zoning and concentric growth-zoning

### 2.1. Shapes and anisotropy of tourmaline crystals

Crystals of tourmaline commonly have a prismatic shape bound by well-defined faces. The prism faces consist of a combination of a hexagonal, trigonal and ditrigonal prisms (Dietrich 1985). Where these forms alternate, the crystal typically exhibits lengthwise striations.

Termination faces are the pedion, trigonal and ditrigonal pyramids of varying steepness, solely or in combinations (Figs 2a–d, Dietrich 1985; Rustemeyer 2003b). Doubly terminated crystals commonly exhibit different shapes on them at the $c+$ and $c-$ axes of the crystal. This is a consequence of one of the most diagnostic properties of tourmaline: its lack of a center of symmetry resulting in a strong anisotropy along $c$, the prism axis (e.g., Dietrich 1985). This anisotropy results in distinctly different properties at opposite poles of the crystal and gives tourmaline its strong piezo- and pyroelectric properties (e.g., Dietrich 1985; Rustemeyer 2003b).

When uniformly heated, one termination of a given tourmaline crystal will develop a positive charge, and the other becomes negative. This charge will reverse upon cooling. Based on this development of charge, the opposite poles are referred to as $c+$ and $c-$ (also named antilogous and analogous pole), where the $c+$ pole is positive during compression along the $c$ axis and upon cooling, and negative when heated or decompressed. These effects are opposite for the $c-$ crystal termination. The polar anisotropy of tourmaline also manifests itself in steeper and more numerous end-faces and a higher growth rate for the $c+$ pole, allowing the poles to be identified in well-formed single crystals in a longitudinal cut of a biterminated crystal (e.g., Dietrich 1985; Rustemeyer 2003b; Van Hinsberg 2006). Further strong compositional differences exist between opposite poles, which express themselves as compositionally distinct overgrowths on opposite ends of the crystal (e.g., Henry and Dutrow 1996).

### 2.2. Sector zones and forms

Owing to differences in interface texture, each crystallographic form of the tourmaline may grow with an individual chemical composition, in many cases, as a distinct color. A sector zone (Dowty 1976; Rakovan 2009) is defined as the volume element of the crystal resulting from the crystallization of a specific form. A form is defined as a set of crystal faces related to each other by a symmetry operation; all faces of a given form have the same arrangement of atoms (e.g., Klein and Dutrow 2007). The simplest example is the pedion in the crystal shown in Fig. 2a, which is a combination of the pedion and the hexagonal prism. In this tourmaline, the pedion face attracts blue-coloring tourmaline, the prism faces attract the yellow one. Thus the blue sector zone from the pedion in Fig. 3a has the shape of the upper half of an hourglass (Van Hinsberg et al. 2006). The sector zone of the prism faces fills the complementary volume; in the slices, it forms the yellow rim zone (which was in the last stages overgrown by a green and blue layer).

### 2.3. Intrasectoral color zones

Tourmaline crystals commonly display a combination with the two trigonal pyramids **o** (large) and **r** (narrow) as termination faces (Fig. 3a, 3b with **r** shown in red). Figure 3b exhibits a large example of such a sliced crystal from the Anjanabonoina pegmatite in Madagascar. The longitudinal cut was reconstructed and completed from the images of the crosscuts. It shows how the pyramid and prism faces crystallized layer by layer. The sector zones of the trigonal pyramid **o** were marked transparent green; they consist of a parallel series of intrasectoral color zones. The crosscut slice in Fig. 3b shows a core area with pyramidal sector zones and a rim area with the sector zones of the prism faces. The horizontal crosscut slice cuts through the inclined intrasectoral color zones of the trigonal pyramid **o**, which form concentric triangles (the narrow face **r** is neglected) in the core area, and through the hexagonal and trigonal prisms **a** and **n**, which form the rim area.

The sequence of intrasectoral color zones indicates the evolution of the color (chemical composition) of a given form during the growth of the tourmaline crystal, whereas sector zoning represents growth at the same time of two (or more) compositions or colors as a result of growth on multiple forms.

⇨

**Fig. 3** Graphic and stack of slices of a tourmaline crystal; **a** – blue tourmaline grew on the pedion while yellow tourmaline grew on the prism faces the first period of growth; **b** – sliced crystal from Anjanabonoina in Madagascar, Ø 15 cm, collection of Michael Benner, Perspective view of the stack of slices, reconstructed longitudinal cut, sector zone of the trigonal pyramid **o** shown in green. **c** – tourmaline slices from Minas Gerais, Brazil, Ø 2–3 cm. The sector zones in the core area illustrate the 'crystal's shape (in grey) at the level of the slice. A corresponding ideal crystal is displayed.

trigonal pyramid o (02.1)
trigonal pyramid r (10.1)
hexagonal prism a (11.0)
trigonal prism n (02.1)
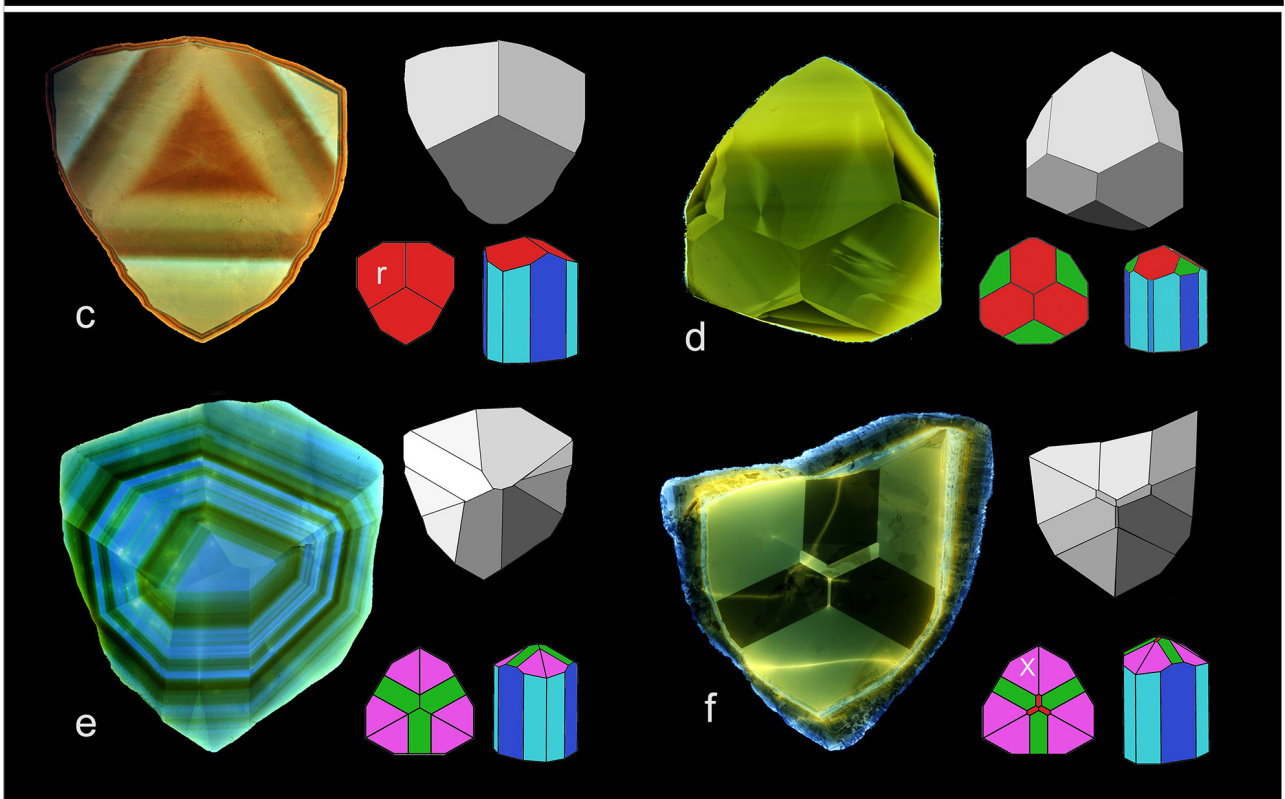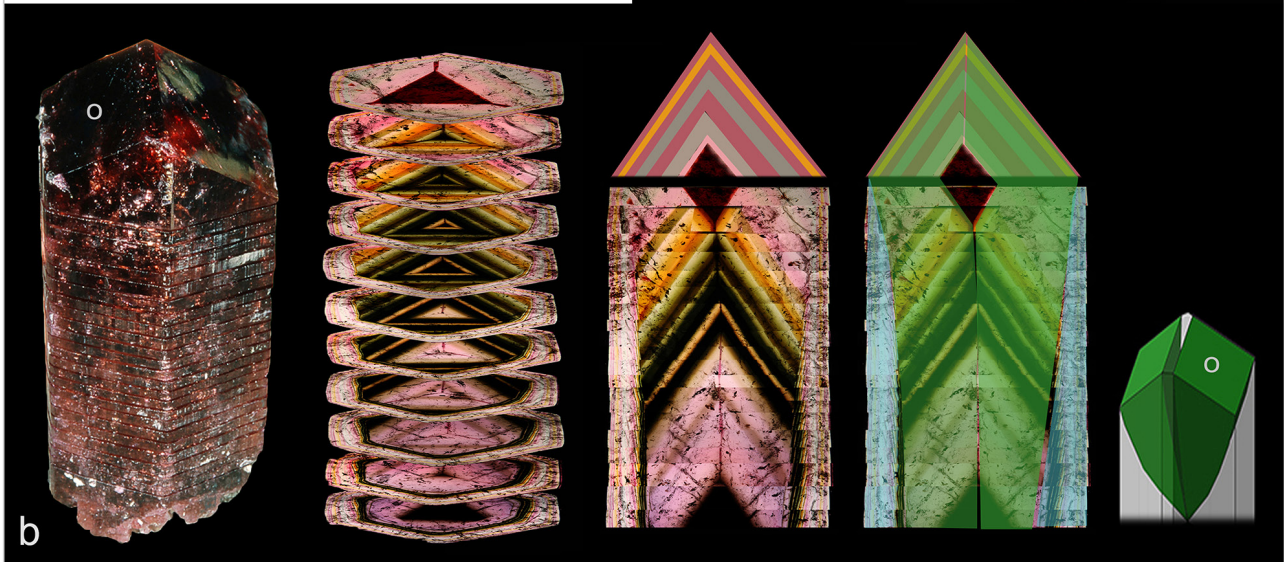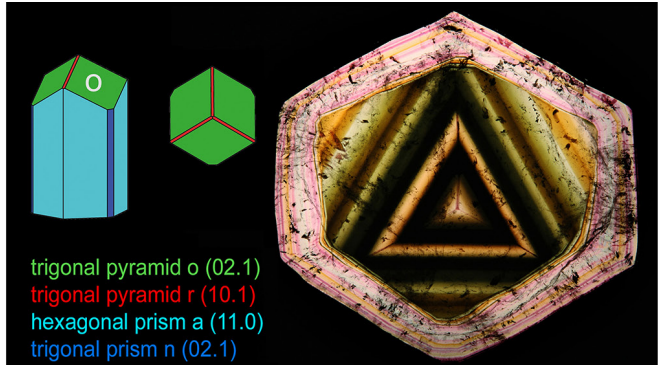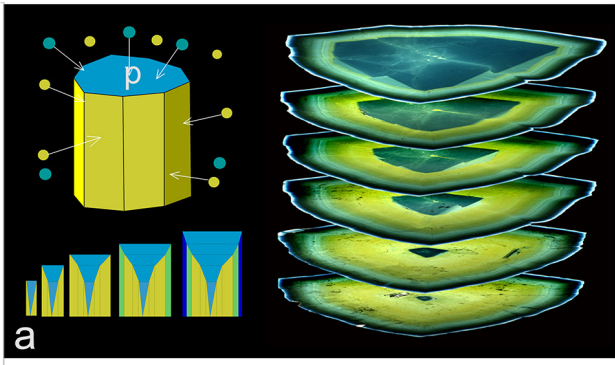
## 2.4. Concentric growth-zones and oscillatory growth

Longitudinal cuts and crosscuts through doubly and singly terminated crystals, as schematically shown in Figs. 2e–o reveal concentric growth zones. Figures 2e and k contain the boundaries of the growth stages. The denser areas indicate the rim zone with the thin layers of the prism faces. In Fig. 3b, the sector zone of the trigonal pyramid **r** and **–r** is marked in grey; in this way, its hourglass structure is emphasized.

Because of a slower rate of growth, the crystal is shorter in the *c–* direction.

Concentric growth zones (Van Hinsberg et al. 2006) are visible in Figs 2g, i and l, where grey color zones have been filled in. If more elements causing a dark coloring are available in the growth medium, darker layers grow on all faces of the crystal (different forms still may have distinct colors). Rapidly alternating thin bright and dark layers form an oscillatory zonation. Such zonation has been debated but is thought to be generated by diffusion-controlled growth in which there is depletion of the surrounding medium in specific chemical components, thus effectively changing the chemical growth environment. This leads to a change in the composition of the newly forming layer as long as replenishment of the surrounding medium is hampered by limited diffusion (e.g., Allègre et al. 1981; Lussier and Hawthorne 2011).

Thus in a longitudinal cut or crosscut, such intrasectoral color-zones define the concentric growth-zones. Such zones are also visible in the crosscut slice in Fig. 2l as concentric triangles in the core area (Fig. 2m), combinations of triangular color-zones with narrow zones in the rim area (Fig. 2n), or combinations of concentric color rings in the rim area (Fig. 2o).

The shape of the tourmaline crystals in Figs. 2e–i is very commonly encountered. In the first period of growth, the crystal has a more equant shape, with comparable rates of growth on the pyramidal and prism faces. As the ratio of the growth rate of the pyramidal faces to that of the prism faces increases continuously. At the final stages of crystallization, only pyramidal faces continue to grow.

## 2.5. Diversity of forms in tourmaline slices

Minerals of the tourmaline group exhibit diversity in possible forms. Numerous trigonal and ditrigonal pyramids with different steepness and orientations can occur (Goldschmidt 1923; Rustemeyer 2003b). This diversity in forms can be documented in tourmaline slices. Figs. 3c–f illustrate some examples. Different colors and different orientations of the intrasectoral color zones indicate the boundaries of the sector zones. This allows one to recognize the crystal's shape on the basis of evidence in the slice.

The slice in Fig. 3e is a good example of concentric growth-zoning. The sector zones of the trigonal and ditrigonal pyramids show strong intrasectoral color-zoning as the crystal grew with both forms incorporating different compositions due to variations in the growth medium. Thus a concentric pattern of colors was formed. The inner intrasectoral color zones of the trigonal pyramids in Figs 3b and 3c also show similar concentric zoning. At first glance, the outer color zones seem incomplete, but thin layers in the rim complete the concentric growth zones.
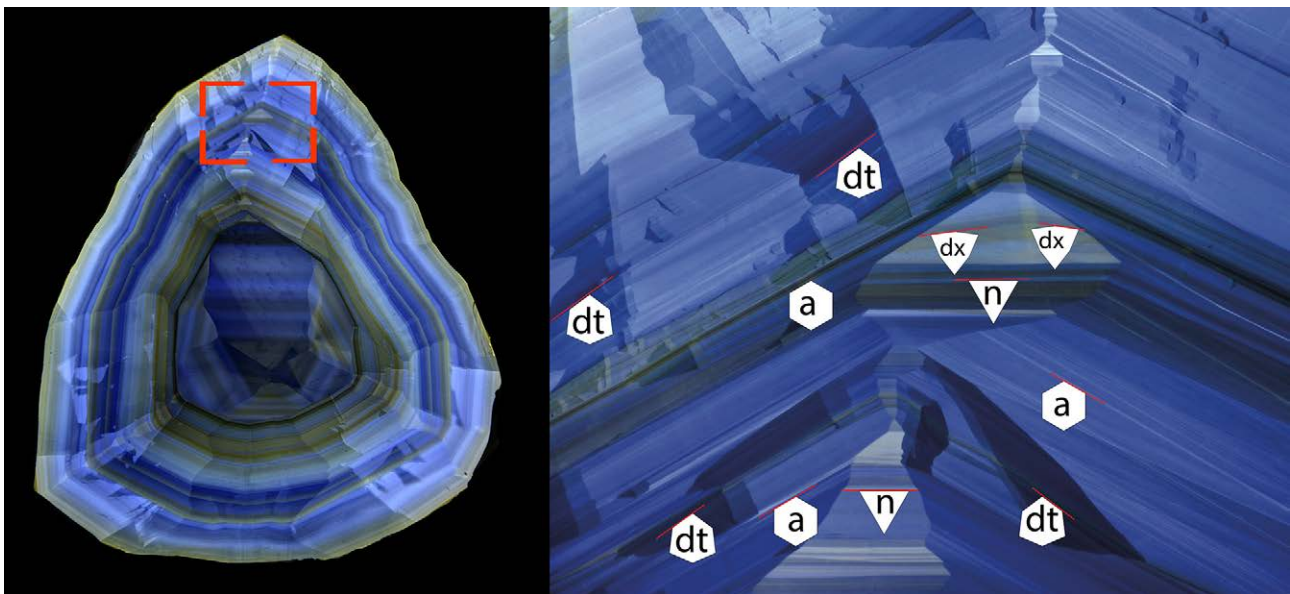


**Fig. 4** Tourmaline crosscut from Minas Gerais, Ø 2 cm, and a detail taken from the rim zone. White profiles of the trigonal prism **n** (01.0), the hexagonal prism **a** (11.0), and the ditrigonal prisms **dt** (21.0) and **dx** (12.0).

## 2.6. Sector zones in the rim area

The rim zone of many tourmaline crystals reveals an impressive and complex array of sector zones and intrasectoral color zones (Fig. 4). This is a consequence of a combination of a multitude of prism forms, which creates the typical striations on the prism faces of most crystals. A reference of orientation is given by the horizontal layers of the trigonal prism n. Its width typically varies strongly. The identification of the prisms was made graphically by insertion of the white profiles of the trigonal, hexagonal and ditrigonal prisms in Fig. 4.

In the last growth phase, in many cases, there is no prismatic growth and no rim at all. Thus, slices in Figs 3e, 5a (section G), or 5a (section E) originate close to the top of the crystal.

## 3. Delta Features

### 3.1. Morphology of simple delta features

A second domain with a distinct color may grow simultaneously within the faces of trigonal pyramids of a tourmaline. Because of their mostly triangular shape and because it is an integral part of a single pyramidal face, the author has called this type of color zone a "delta feature" (Rustemeyer 2003b, 2011, 2015a). The examples of slices in Fig. 5a provide an impression of the diversity of shapes of such features. The most common delta features start at a seed point in the sector of a trigonal pyramid and spread downward toward the edges of the pyramid faces with the prism faces, shaped more or less as isosceles triangles with variable angles (Fig. 5b).

In many cases, a series of slices is necessary to understand the full three-dimensional shape of the entire feature. In the stack of slices in Fig. 5b, the sections of the delta feature are yellowish. An extrapolation of these areas shows that the delta feature is embedded in the crystal-like inclined wedge-shaped pieces of pie, the bottom and top faces of which are parallel to the pyramidal face of the hosting sector zone. When a tourmaline crystal is cut in horizontal slices, a large delta feature within the crystal is also divided and visible on several levels. The lowest slice contains the lower rear part of the wedge, which looks like a truncated cone that touches the rim zone. The uppermost slice contains a triangle corresponding to the tip of the wedge-shaped delta feature.

A longitudinal cut through the middle of a crystal (Fig. 5cA) and an additional crosscut provide complementary information (Fig. 5cB). The longitudinal section confirms that the delta features are parallel to the pyramid face in which they grew. Numerous parallel delta features could indicate oscillatory growth. The strong dichroism of the crosscut and longitudinal slices in Fig. 5c reveal blue and brown colors, which are typical for dark crystals of tourmaline.

### 3.2. The delta feature as an integral second colored domain of a pyramidal face

When screening thousands of tourmaline crystals under full reflection in parallel lighting, a condition in which very fine surface features can be observed (Rustemeyer 2003b), there is no sign of a delta feature with triangular vicinal faces. Therefore, longitudinal cuts of twenty crystals with smooth and glossy pyramidal faces were made to find a tourmaline with a delta feature just below the surface of the trigonal pyramid. One such sample was identified (Fig. 6a). The two pieces with the pyramidal faces were glued on a glass platelet and a thin section was prepared. The thin section contains the corresponding delta feature. In this way, the delta feature can be shown to be an integral part of the trigonal pyramid without visible evidence on the surface.

### 3.3. The diversity of shapes of delta features

Figures 6b, c and d show crosscuts with a superposition of several delta features nucleating at different points. Interestingly, a gap in the color of the hosting tourmaline commonly remains between two delta features. The typical ellipsoid pattern separating delta features could result from surface diffusion of the chromophores. However, the dark brown delta feature grew complexly, as has been found in numerous crystals. In order to give a three-dimensional impression of the morphology of the whole delta feature, detailed pictures from the five slices have been stacked to give a perspective view (Fig. 7).

Many nucleation points offered growth options for the delta features in Fig. 6e; most delta features have remained small. Some look as if they have been strung into a garland.

The delta features in Fig. 6f look fractured as the color goes "*to and from*" across the boundary. This is because the brown or yellow inner space of the delta feature is irregularly structured. In addition, a triangular seam envelops the delta features in Figs 6f and g. At higher magnification, this seam consists of many minute elongate delta features.

A frequently occurring type of a delta feature develops from the point of nucleation not only as a triangle pointing downward but also as a counter triangle pointing upward on the pyramidal face **o** (Figs. 6h and i). The latter fades without contour into the surrounding face. This
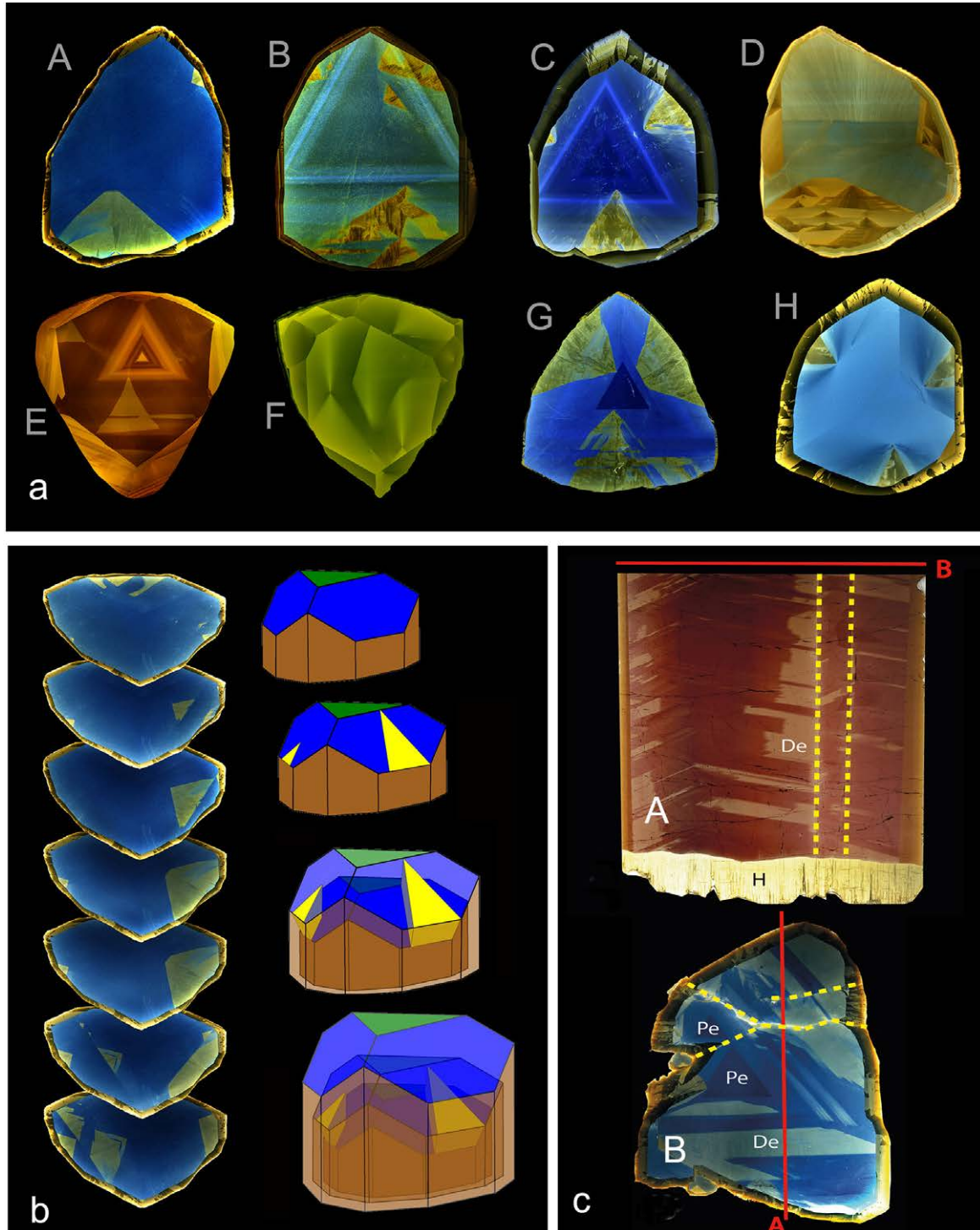
**Fig. 5 a** – Tourmaline slices exhibiting the diversity of intrasectoral delta features, A, C and G from Skardu, Pakistan, B, D, F, H from Minas Gerais, E from Madagascar; Ø 1.8–3 cm. **b** – Left side: Stack of tourmaline slices with yellowish delta features, (Skardu, Pakistan, 28 mm in diameter). On the right side: development of the delta feature as a triangular second color domain within the face trigonal pyramid. The delta features form layer packages that are arranged in the crystal-like inclined triangular wedge-shaped pieces of cake (parallel to the surface of the trigonal pyramid). In many cases, one horizontal slice exhibits only a part of a larger inclined delta feature. **c** – Slice **A** parallel (brown) and slice **B** perpendicular to the *c* axis from the same schorl crystal with delta features (different colors due to dichroism), sample from Kunar Valley, Afghanistan, Ø 3.5 cm. The red lines indicate the orientation of the cuts. The two sector zones from pedion faces **Pe** and the border lines (dotted yellow lines) indicate that the crystal consists of three parallel crystals. In slice A, delta features can be seen as light brown areas that slope upward from the edges, and in slice B, as yellowish areas. The horizontal slice B cuts through several of the inclined delta features. At the bottom, the red–brown area ends with an irregular border, which is typical of a fractured surface. This was later overgrown by numerous fibrous yellowish crystals (H).
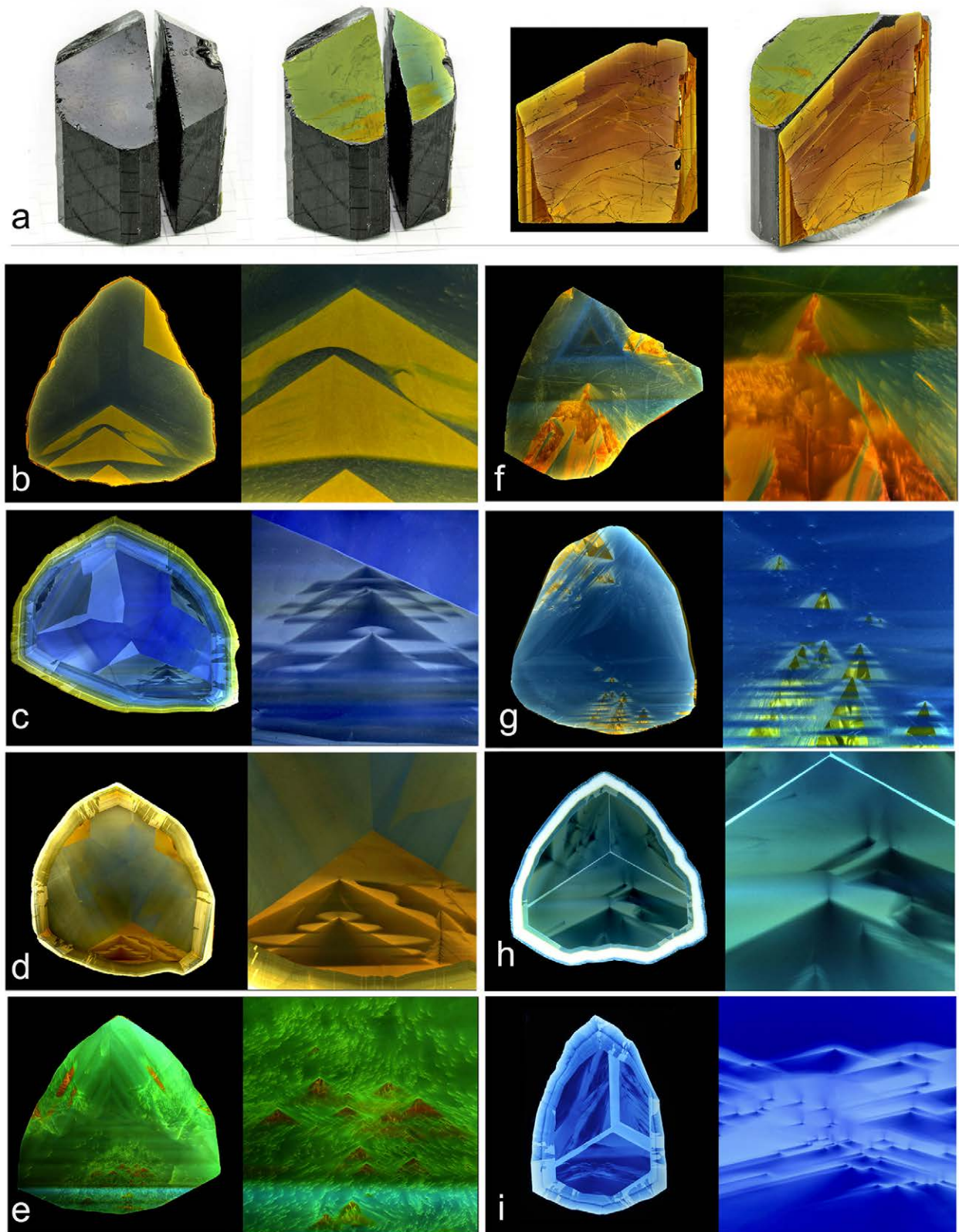
**Fig. 6 a** – Tourmaline crystal with a delta feature in a crosscut and in a thin section made from the surface layer of the pyramid; Skardu, Pakistan, Ø 23 mm. **b–i** – Tourmaline slices with diverse delta features and a corresponding detailed view, Minas Gerais, Brazil, Ø 18–27 mm; **b–d** – view with several overlying delta features; **e** – Numerous points of nucleation for the delta features; **f, g** – delta features which look fractured with a triangular seam, **h–i** – delta features with a counter triangle ("volcanoes with an ash cloud").
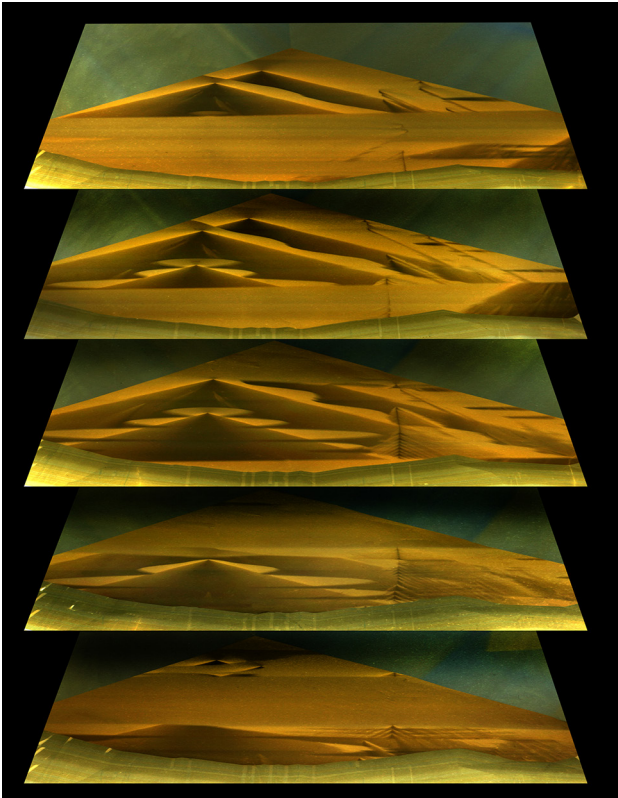
Fig. 7 Perspective view of the detailed illustrations prepared from the series of slices corresponding to Fig. 6d. The series gives an impression of the ellipsoidal space separating the three overlain delta features.

creates an image that appears like a volcano with an ash cloud. Tourmaline crystals with trigonal pyramids **o** and **r** may contain two different delta features in each form; the ones within **r** exhibit a steeper angle (Fig. 8).
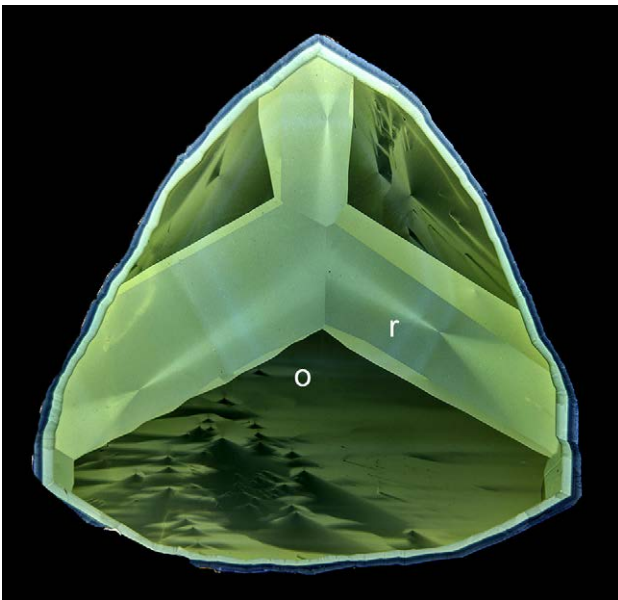


Fig. 8 Two different types of delta features in the pyramids **o** and **r**, in a crystal from Minas Gerais, Ø 22 mm.
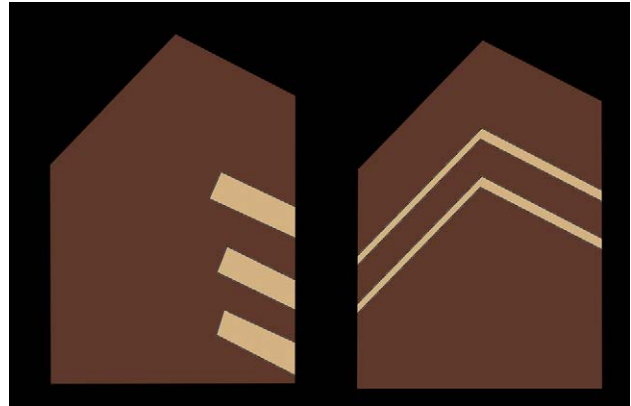


Fig. 9 Intrasectoral delta features as an alternative to complete pyramidal color zones.

Points of nucleation are commonly submicroscopic. Visible points may be the rim of a vacancy in the crystal, a dislocation, an inclusion, or an edge of the pedion intersecting a trigonal pyramid. A multitude of parallel delta features in longitudinal cuts indicates an oscillatory mechanism of growth.

Delta features seem to be an alternative to complete pyramidal color zones (Fig. 9). This suggests that the growth of delta features is the result of a simultaneous oversaturation of two color domains with limited miscibility but the same affinity to the surface. The following parameters could play a role in the development of the different shapes of delta structures:
– the concentration, the relative oversaturation and relative diffusion rate of the coloring building blocks compared to those of the host pyramid face,
– the number of nucleation points and
– the steepness of the pyramidal face.

This study is based on visible features within tourmaline slices. The chemical composition and structural differences of the delta features and the hosting pyramidal sector zone remain to be analyzed.

## 4. Healing phenomena after fractures

Sometimes tourmaline crystals get fractured and/or broken off. The causes of the fractures are probably (micro/macro) tectonic events, which shocked or sheared the content of a pegmatite pocket. Tourmaline is weaker in the $c$ direction, and it is easy to pull apart (*i.e.*, it has a low tensile strength). Wherever shear or extension forces exist, the tourmaline will break, with most fractures roughly perpendicular to the $c$ axis. Not uncommonly, the fractures heal by the growth of tourmaline of a different color and/or composition (Fig. 10a; e.g., Henry et al. 2003), which shows that there has been an influx of fluid with differing compositions into the pocket. Because of the differences between the $c+$ and $c-$ poles, the over-
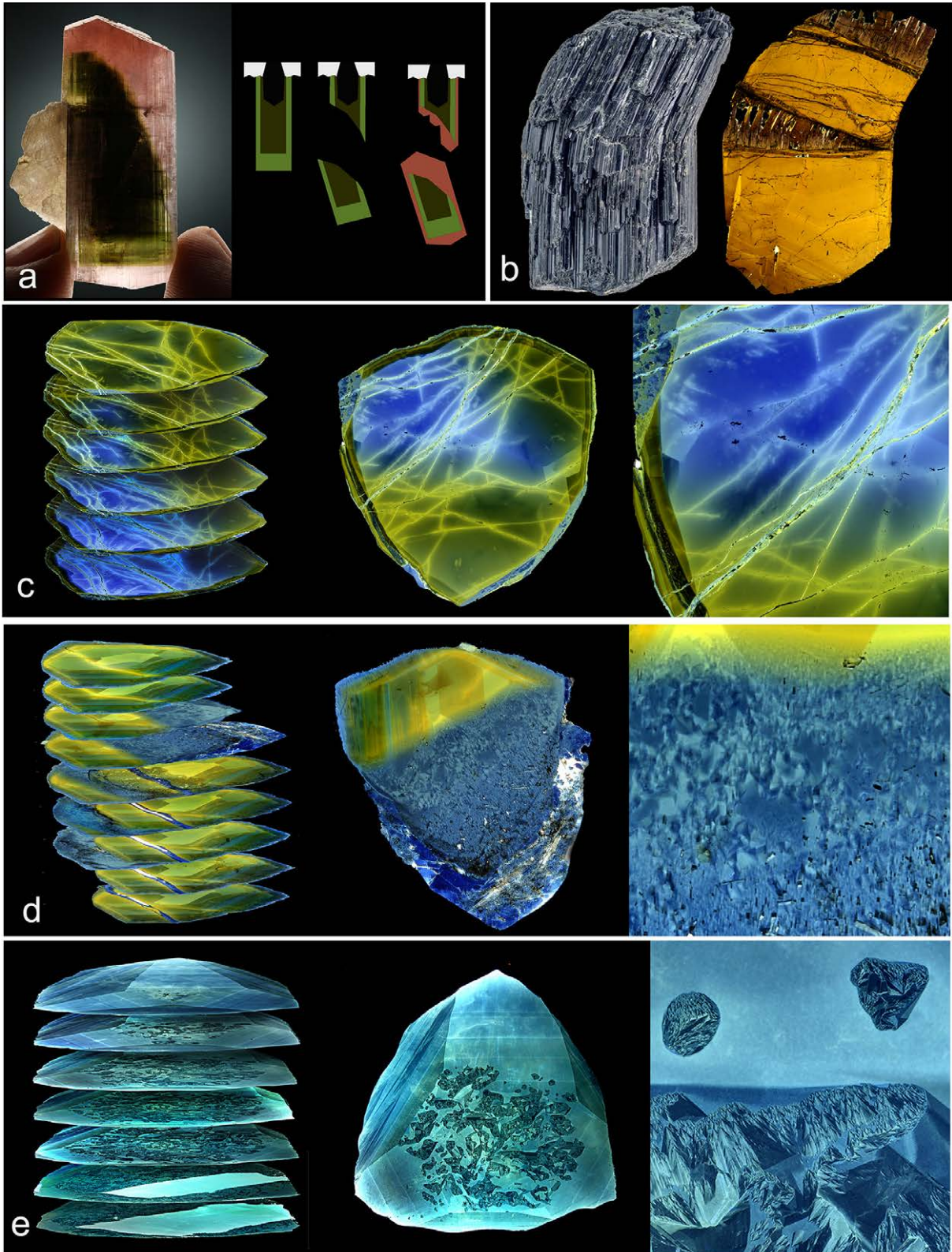
**Fig. 10 a** – A green crystal of tourmaline breaks off and falls on a layer of clay. Its upper antilogous fractured termination continues to grow substantially faster as a red tourmaline according to the polarity of the crystal. The fracture heals and a perfect doubly-terminated crystal develops. Kunar valley, Afghanistan. **b** – Broken and healed schorl with the corresponding longitudinal cut. The small crystals responsible for the healing are dark brown. Shigar valley, Pakistan, 7 cm long. **c–e** – Fractured, healed and sliced crystals, with detailed illustrations, from Minas Gerais, Ø 32 mm, 15 mm, 38 mm.
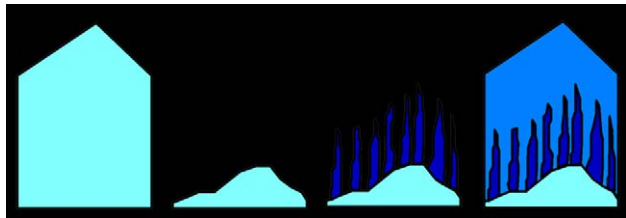
**Fig. 11** Fracture and healing process of the crystal in Fig. 10e. At first, complex bundles of triangular needles grew, then embedded in homogeneous material.

growths are commonly only (or predominantly) on one fracture surface. Crystallization on fractures is observed in numerous crosscuts of dark tourmaline crystals from many locations (e.g., Rustemeyer 2003b, 2011, 2015a, 2017, 2018, 2019 a, b). In many cases, the newly-formed material is differently colored and heterogeneous. The boundaries of the areas of new growth are as irregular as the shards of a broken crystal (e.g., Henry et al. 2003; Rustemeyer 2003b, 2015a). In many cases, there is no sign of this new growth on the surface. The term "healing" seems a justified term.

A clay-rich substrate presence in cases of pocket rupture can help in keeping broken fragments juxtaposed so that the healing can proceed. Figures 10b and 10d show fractured and healed crystals, where the shards have been inclined and offset before healing.

Figure 10c shows a sliced tourmaline with many healed fractures. The detailed image shows that some of the fractures go through the rim zone; others end before the rim, a sign of at least two episodes of breakage. A fractured surface offers many points for the nucleation of small, oriented crystals.

Where a tourmaline grows in only the longitudinal direction, a hairy fur of many parallel crystals is formed. If the opposite fractured surface is close by, the small needle-shaped crystals grow toward each other and interlink. A decreasing amount of tourmaline manages to enter into this tight space; in this way, small open spaces remain in the zone of healing (Fig. 10b). Despite these

voids, the crystal will look quite compact from the outside. An oriented overgrowth of tiny needles on a fracture surface can be classified as a subdivision phenomenon. The effect is described in Section 6.

In rare cases, the area of healing produces what looks like islands in the sea. Figure 10e shows an example of such a sliced crystal, in which the first stage of healing produced complex bundles of tiny tourmaline crystals, which were later embedded in a uniform tourmaline matrix (Fig. 11).

## 5. Healing phenomena after corrosion

A crystal of tourmaline growing in a pocket may begin to dissolve if the ambient fluid becomes undersaturated (London 2016), of different composition (Dutrow and Henry 2000), or alkaline (Henry and Dutrow 1996) (Fig. 13; London 2016). This corrosion commonly occurs along defect-rich areas and can lead to various shapes and forms (Figs 12, 14). Numerous etched tourmaline crystals in the collection of the author originate from Minas Gerais in Brazil, some are from the Shengus area in Pakistan (Rustemeyer 2003b, 2011, 2015a) and a few have been found in a pegmatite close to Herzogau, Bavaria, Germany (Rustemeyer and Prögler 2019).

Doubly terminated corroded crystals will exhibit different features at their terminations (Fig. 15). The antilogous pole is more intensely corroded. Deep etching of trigonal pyramids and prisms is commonly the result. The more resistant analogous pole may build a stripe pattern in the direction of the three sharper edges of the cross-section of the crystal. In many cases, the surrounding fluid eventually becomes supersaturated, and the tourmaline continues to crystallize, in many cases with a different color. The crystal may heal so perfectly that no sign of this corrosion and healing history is evident from the outside (Fig. 12). The surprise is all the greater when one finds clear traces of etching and healing in the crystal upon scrutiny of the slices. A good indicator of such a process is the presence of trigonal boundaries in
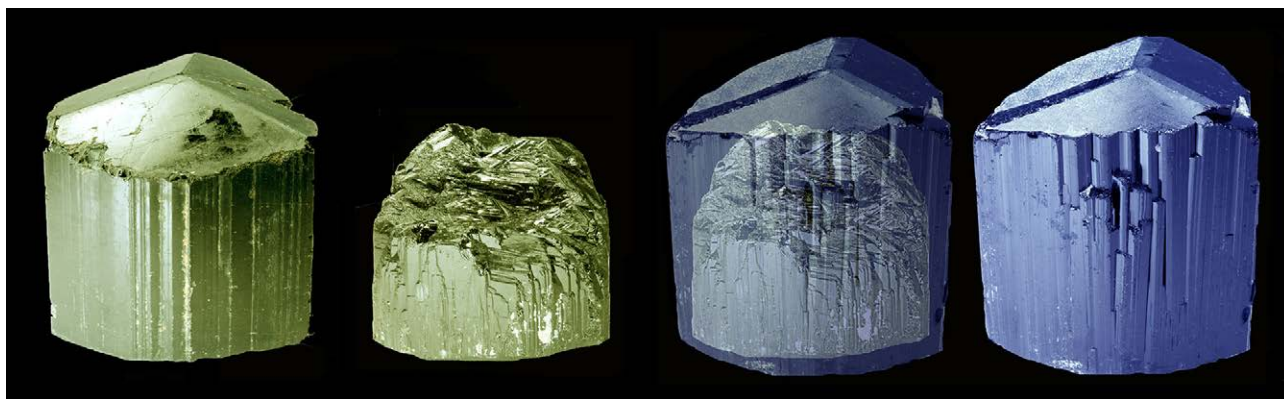


**Fig. 12** A yellowish tourmaline is corroded naturally and then healed with a blue tourmaline (scheme based on three crystals from Minas Gerais, Ø 4–6 cm).
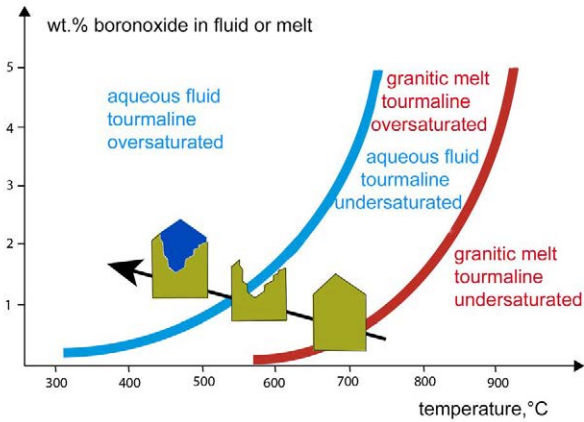
**Fig. 13** Areas of undersaturation and oversaturation in melt and aqueous solution; in the overlapping area, corrosion of tourmaline crystals is possible (after London 2016).

the healing areas, as in most cases, trigonal prisms and pyramids are the preferred forms that are etched from the initial crystal. In many samples, tiny needles resisted the corrosion of the initial crystal.

The inner architecture of the healed areas depends on the process of overgrowth; three different variants have been discovered (Fig. 16). Most of the samples with features of healed corrosion in the slices originate from Minas Gerais in Brazil, much less are from the Shengus area (Rustemeyer 2003b, 2011, 2015a).

### 5.1. Overgrowth on the corroded pyramidal faces only

During the healing process, the new tourmaline may continue to crystallize at a high rate of growth in the direction of the *c* axis on the numerous faces of trigonal pyramids forming the corrosion relief. Each different form attracts chromophores differently. As a result, a thick layer may form, in which the corroded surface is transformed into a pattern of colors. Thus the corrosion pattern of the analogous and antilogous poles can be retained in those layers (Figs 16a, b). In many instances,
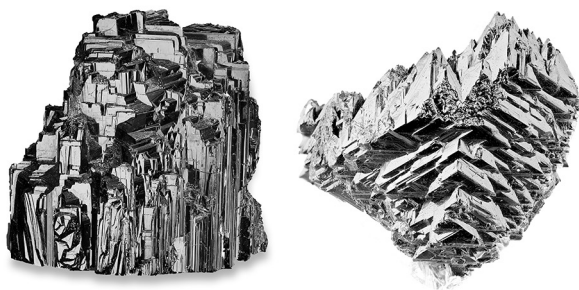
the overgrowths on trigonal etch-pits from the antilogous pole define a triangular pattern.

### 5.2. Overgrowth on prism and pyramidal faces

If the prism and pyramid faces have comparable growth rates once crystallization restarts, a type of inner rim can appear along the prism faces. In Figure 16c, tiny needles with prism faces and steep pyramids have been etched out of the original yellowish crystal. These structures have been overgrown with an oscillatory layer of a green tourmaline (see the detail in Fig. 16c). The last healed layer consists of blue tourmaline. The crystal of these slices originates from a pegmatite close to Windorf, Bavaria, Germany (*in prep.*).

### 5.3. Overgrowth of needle-shaped crystals later form an "island-in-the-sea" arrangement

The habits that develop in the zone of healing are similar to those that develop on a fracture surface. An oriented overgrowth with tiny parallel needles on a corroded surface can be classified as a subdivision phenomenon. The effect is explored in the next section (Fig. 17b). In the crosscut, these can be seen as finely triangular "islands". The much more uniformly colored "sea" area crystallized later and needles were embedded in it (Fig. 11).

## 6. Subdivision phenomena

There are tourmaline crystals in which a single crystal is transformed into a bundle of parallel or subparallel subindividual crystals. Here these are attributed to subdivision phenomena. Six different subdivision mechanisms have been discovered based on analyses of tourmaline slices (Fig. 17). Many of the subdivision phenomena were discovered in tourmaline crystals from the Erongo
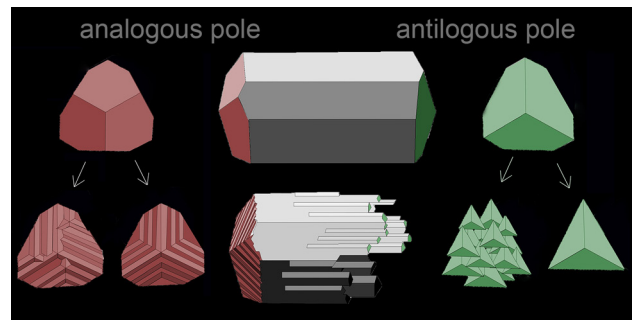


**Fig. 14** Complex shapes of strongly corroded tourmaline crystals from Sta. Rosa Mine, Minas Gerais, Ø 3.5 and 5 cm.



**Fig. 15** Doubly terminated crystals develop features of corrosion at the poles, with distinct features on the analogous and the antilogous pole (Rustemeyer 2015a).
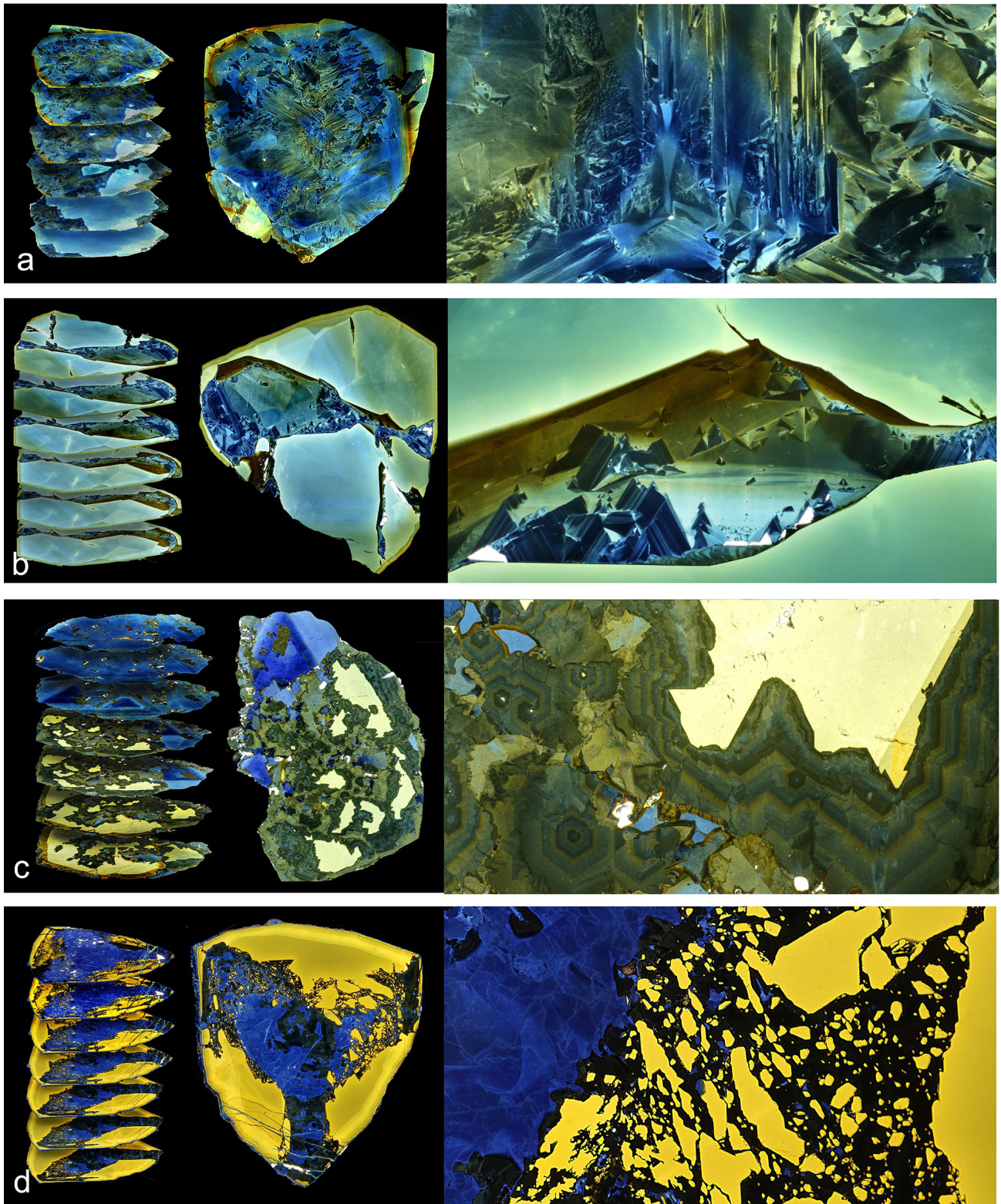
**Fig. 16** Four types of features in corroded and subsequently healed tourmalines, illustrated in a stack of slices, a representative slice and a detailed view (3–5 mm wide). **a** – healing pattern at an analogous pole with trigonal oriented stripes, Minas Gerais, Ø 3 cm. **b** – pattern of healing at an antilogous pole with triangular features, Minas Gerais, Ø 3 cm. **c** – pattern of healing with lateral overgrowth of prisms and steep pyramids with green layers, Windorf, Bavaria, Germany, Ø 2 cm. **d** – healing pattern involving deeply etched holes with many resistant needle-shaped parts, Minas Gerais, Ø 2 cm.
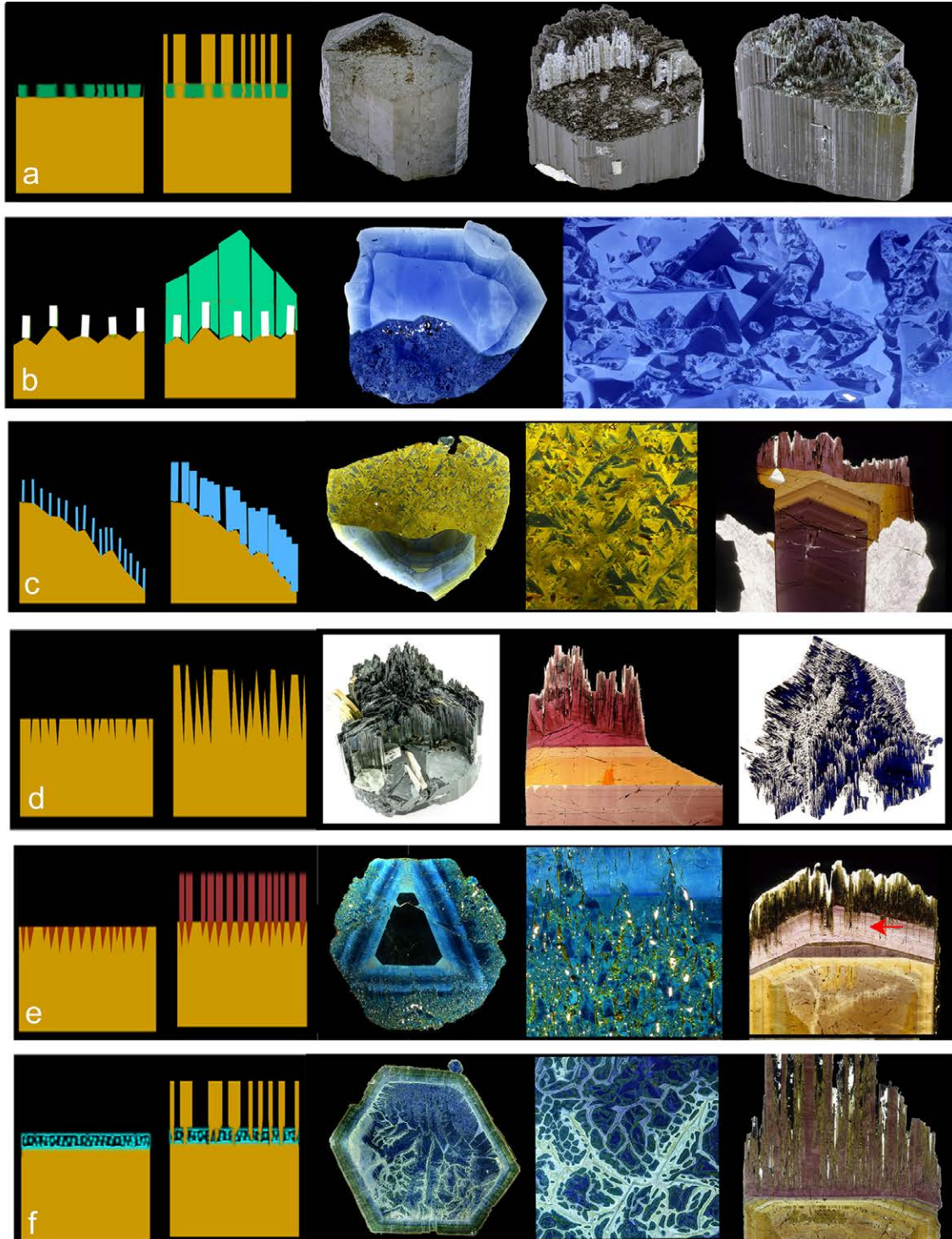
**Fig. 17** Six causes of the subdivision are shown by a schematic, natural example and close-up views. **a** – Oriented overgrowth on a porous barrier layer, two crystals from Erongo, Namibia, and on the right side, from Minas Gerais, Brazil, Ø 3–5 cm. **b** – Needle-shaped overgrowth on a corroded surface, slice with dark blue healing area from Minas Gerais, Ø 2.2 cm, on the right side a 2 mm wide detail from the healing area. **c** – Needle-shaped overgrowth on a fractured surface, brownish healing area in a slice from Minas Gerais, Ø 2.5 cm, detail, 2 mm wide, right side: longitudinal slice from Skardu, Pakistan, 2 cm wide. **d** – Trigonal subdivision, crystal from Minas Gerais, Ø 5 cm with longitudinal and crosscut. **e** – The second generation of needle-shaped tourmaline starts to grow within a homogeneous tourmaline layer, visible as a granular structure in a crosscut from Erongo, Namibia, Ø 3.5 cm with 3 mm wide details. On the right side, the phenomenon is marked with a red arrow in a longitudinal slice from Erongo, 3 cm wide. **f** – A thin layer of skeletal and dendritic tourmaline, a crosscut from Erongo, Namibia, Ø 3.5 cm and a 5 mm wide detail exhibit the skeletal network structure. In a longitudinal cut of a crystal from the same pocket (right side), the skeletal zone is the basis of the needle-shaped crystals.

mountains in Namibia (Rustemeyer 2003a, b, 2011, 2014a, 2015a, 2022)

## 6.1. Subdivision by a partially open barrier layer

The initial "mother" tourmaline crystal may become coated with a barrier layer. Open areas in this layer allow an oriented overgrowth with "daughter" crystals. Examples of such crystals showing a partial overgrowth of termination faces are shown in Fig. 17a. Such a partial overgrowth is commonly observed in minerals like quartz, with a barrier layer provided by iron oxide (Rustemeyer 2009), fluorite or calcite (Rustemeyer 2018).

## 6.2. Subdivision by nucleation at a point on a corroded surface

Figure 17b shows an example of a needle-shaped overgrowth on a corroded surface. In this crosscut, the darker bluish area is the healed zone. The detailed picture shows that bundles of tiny dark blue parallel needles grew in the first step. In the second step, a light blue tourmaline filled the space between the needles and created an "island-in-the-sea" array.

## 6.3. Subdivision by nucleation at a point on a fracture surface

The crosscut in Fig. 17c shows the greyish blue initial crystal with a typical irregular border of a broken tourmaline shard on the bottom. The healed zone's brownish area consists of several interlocked parallel crystals. The detailed image shows blue triangular faces, which are interpreted as pedion faces combined with brown pyramidal faces. The right image in Fig. 17c shows a longitudinal cut through a fractured tourmaline, which then was overgrown with parallel needles.

## 6.4. Trigonal subdivision

With trigonal subdivision, the tourmaline crystals develop deep fissures with a trigonal habit. A strong trigonal subdivision splits off parallel lamellae at the terminations of the crystal. Probably the fissures develop from lattice defects. In Fig. 17d, a tourmaline crystal with strong trigonal subdivision into a clear lamellar structure is shown. From a second similar crystal, a longitudinal cut and a series of crosscuts were made, one of which one is presented here. In numerous crystals, trigonal subdivision produces a multitude of shorter lamellae.

The second example of a tourmaline crystal with trigonal subdivision is from the Erongo Mountains in Namibia. The top area of the crystal shown in Fig. 18 is displayed in Fig. 19 as a detailed image from the longitudinal cut and crosscut. The trigonal subdivision occurs here in the transition area of an iron-rich tourmaline to an iron-poor species like foitite and rossmanite (Boudreaux 2014; Falster et al. 2018). The change in unit-cell parameters may be a trigger for the trigonal subdivision.

## 6.5. Subdivision by a second tourmaline phase

Figure 17e shows on the right side a longitudinal cut through a tourmaline from the Erongo Mountains. The growth of a second dark brown phase can be observed within the uppermost bright violet brown pyramidal sector (red arrow). The dark brown material builds the next zone of needle-shaped parallel crystals. The crosscut and the detail in Fig. 17e show that the clear sector-zone boundaries are dissolved, and the subdivision effect started before the pyramidal face was completed (Rustemeyer 2003b, 2015a).

## 6.6. Subdivision by an intermediate skeletal and dendritic layer

A thin skeletal and dendritic layer on a pedion face of a tourmaline crystal may induce a subdivision into many parallel crystals. Such thin skeletal layers were discovered in numerous tourmaline crystals from the Erongo Mountains in Namibia, from which many different kinds of parallel and subparallel crystals have been described (Rustemeyer 2003a, 2014a, 2015a, 2019b; Boudreaux 2014). Furthermore, research on the morphology of skeletal and dendritic overgrowths, which is the topic of the next section, shows that parallel crystals commonly develop on the branches of the overgrowth. This finding helped recognize the skeletal and dendritic nature of the thin layers, shown in Figs 17f and 18 (section B), in which they form a greenish network.

# 7. Skeletal and dendritic crystals

Skeletal or dendritic crystallization occurs where the supersaturation of the fluid is high and the diffusion rate is low (Sunagawa 2005). Typically, skeletal crystals of halite, sulfur and bismuth, among others, continue to grow on the edges only and adopt the well-known hopper morphology (e.g., Rustemeyer 2018). The author has not yet encountered a crystal of tourmaline with a hopper morphology. Rather, skeletal tourmaline crystals are shaped like tubes, in most instances filled with quartz and feldspar, and only rarely formed within an open space. Single-crystal dendrites grow as irregular arms inside and outside such a tube, forming a three-dimensional
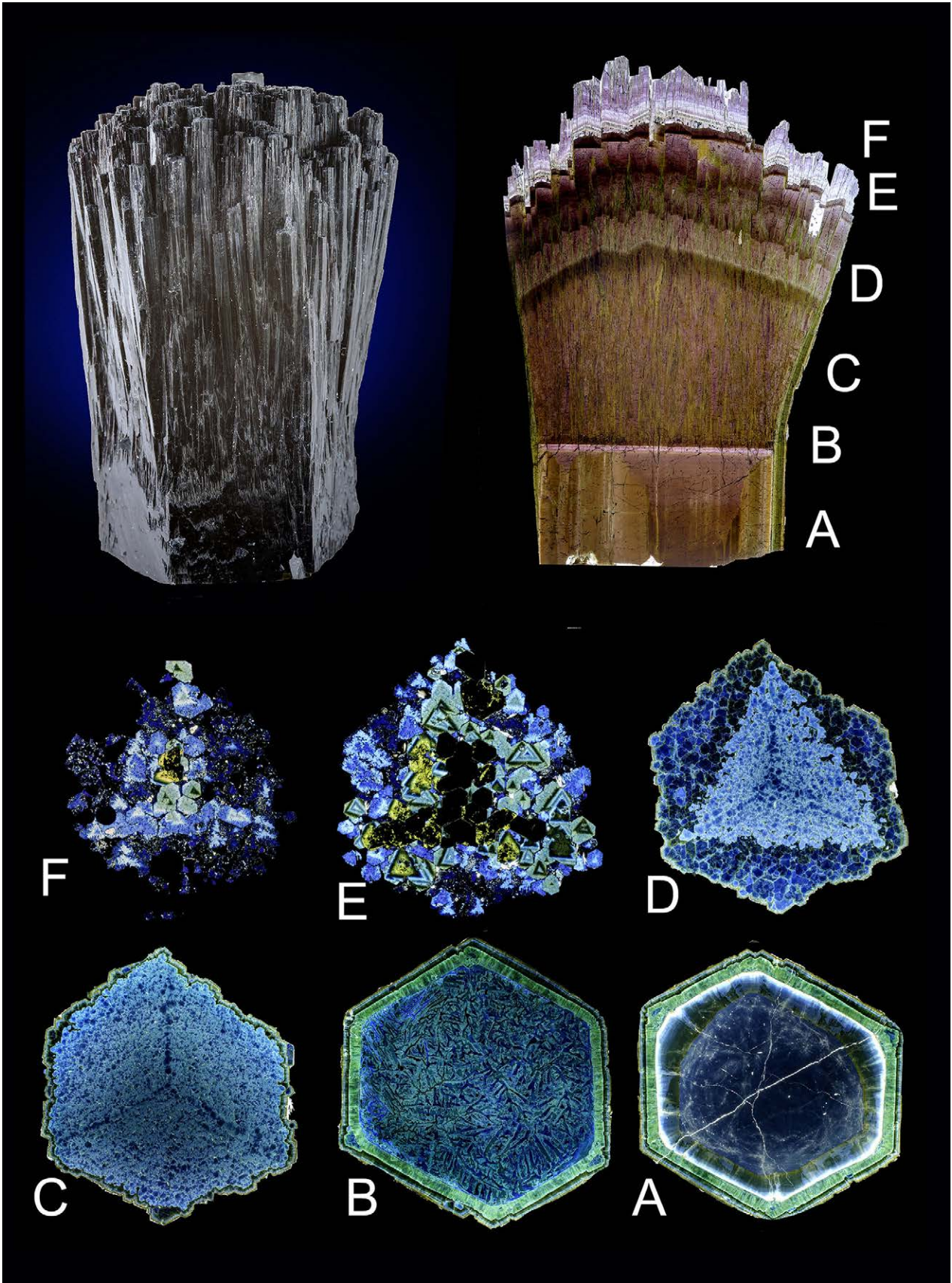
**Fig. 18** Detailed illustrations of the top of the crystal in Fig. 19, above the crosscut and below the longitudinal cut, 6 mm wide.
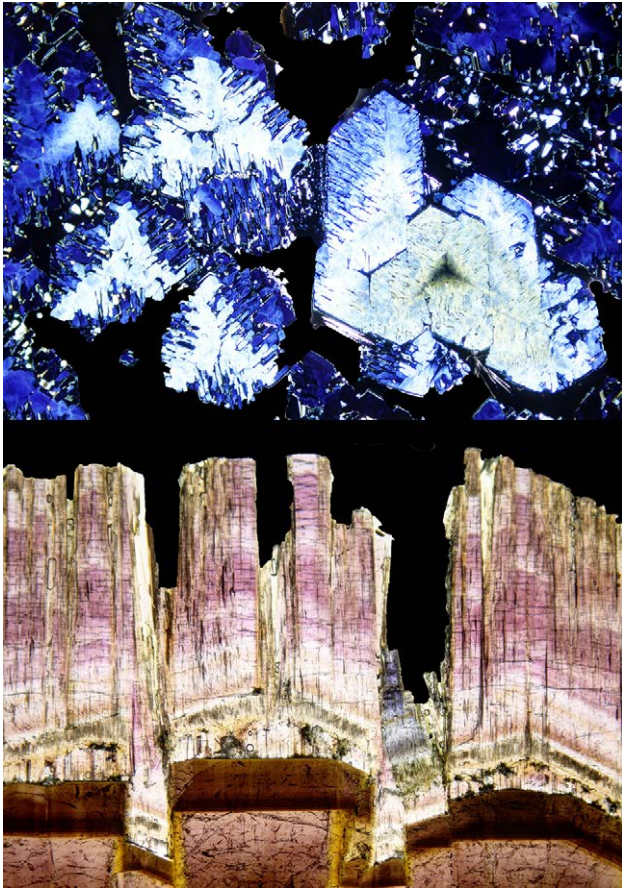
**Fig. 19** Tourmaline from Erongo, Namibia, with subparallel subdivision, above as crystal and longitudinal cut, below as crosscuts taken at different levels A–F, Ø 2.5 cm.

network. Single-crystal dendrites also occur embedded in quartz, feldspar and mica.

Figure 20 provides an overview of the cross sections of typical crosscuts of skeletal and dendritic tourmaline, with and without quartz. In all cases, the different colors of the sector zones in the crosscuts allow one to distinguish clearly the pyramidal skeletal and dendritic growth in a longitudinal direction and the prismatic dendritic growth in a lateral direction. In many cases, a later overgrowth fills the space of the fragile three-dimensional dendritic structure. Common principles governing morphological growth of skeletal and dendritic individuals were discovered in freely crystallized skeletal tourmaline, parallel aggregates, and graphic intergrowth of tourmaline with quartz and feldspar. This will be illustrated with typical examples.

## 7.1. Freely crystallized skeletal crystals

Figure 21 shows two skeletal crystals of tourmaline from Erongo, Namibia. They formed not only as a tube along the prism faces, but also produced an irregular array of lamellae within the tube. The corresponding crosscuts and longitudinal cuts indicate that this is a skeletal overgrowth on a pedion face (Rustemeyer 2018).

Longer tubular skeletal crystals of tourmaline were found about ten years ago in the Apatite pocket close to the Amerika Quarry, near Penig, Saxony, Germany (Rustemeyer 2014b, 2018). Figure 22a shows the crystal, the stack of crosscuts and one typical slice. The skeletal
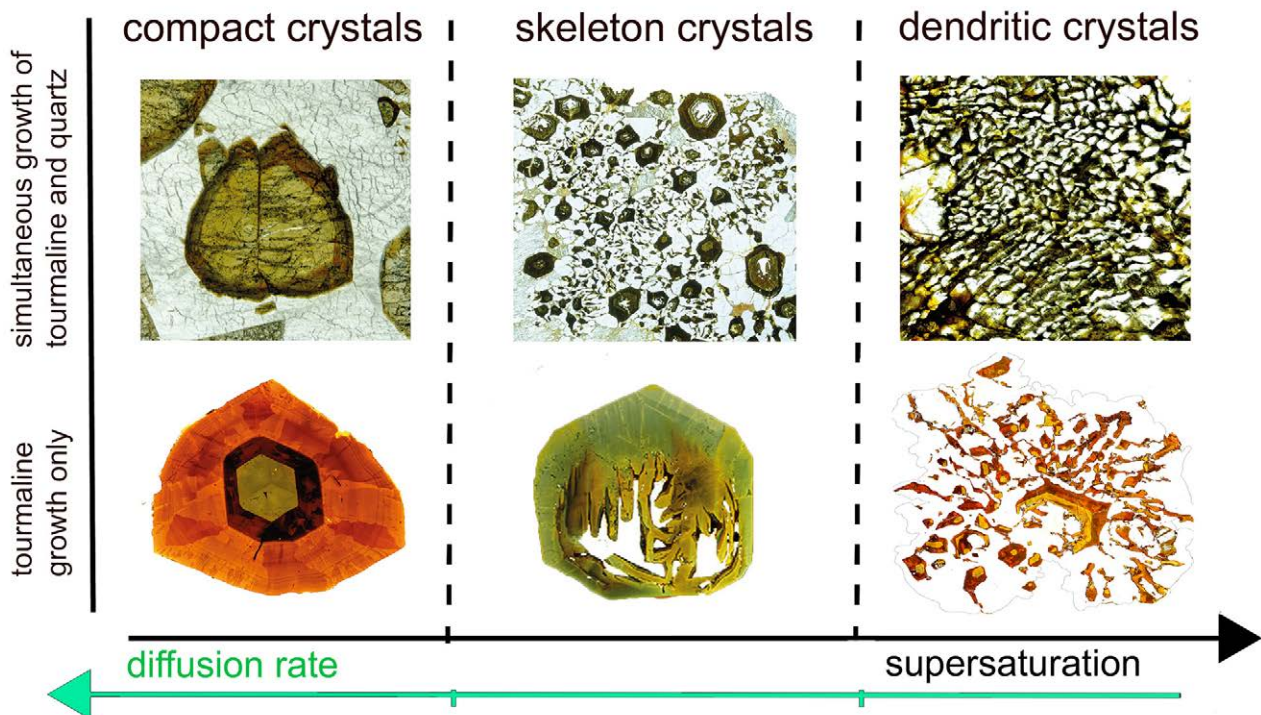
**Fig. 21** Two skeletal tourmaline crystals from Erongo, Namibia, Ø 2 cm, with the corresponding crosscut and longitudinal cut.

crystal is the yellowish ring in the center; it was formed from the prism faces and widened toward the top. Some dendritic lamellae have grown toward the center. A brown rim forms a layer around the outer ring. The core, shown as white, is an open space.

## 7.2. Tubular skeletal crystals in quartz matrix

Quite large tubes of tourmaline, first described by Credner (1875) and Rustemeyer (2014b, 2018), can be found in a pegmatite close to Wolkenburg. They reach 40 cm in length and 2 cm in diameter. Figure 23 shows a longitudinal cut through one of these tubes in which the skeletal arrays are entirely embedded in quartz and feldspar. Each arm widens in the direction of growth. Additional crosscuts monitor the dendritic arms inside and outside the hollow ring of the skeletal tourmaline crystal.

## 7.3. Freely crystallized hollow skeletal tourmaline with monocrystalline dendritic overgrowth and parallel satellite crystal

Figure 22b shows a series of crosscuts of a typical skeletal tourmaline with a yellow tube in the center (the left slice is the lowermost, the right one the uppermost) which indicates a skeleton core. Near the top, the skeleton's

⇦

**Fig. 20** Typical skeletal and dendritic tourmaline shown in crosscuts with and without quartz. Skeletal and dendritic crystallization occurs where the fluid's supersaturation is high and the diffusion rate is low.

tube is transformed into a bundle of dendritic arms. At a later stage, bluish tourmaline overgrew the fluffy array. A similar effect can be seen in the series illustrated in Figs 22c and 25a: a dark skeletal crystal in the center gives way to a bundle of dendritic arms. Laterally, a three-dimensional network of dendritic arms starts at the edges of the crystal. Somewhat later, quartz nucleated and grew on the dendritic tourmaline. In this way, the fragile dendritic structure was embedded in quartz. Finally, a ring of parallel satellite crystals grew on the lateral exposures of the dendritic tourmaline. From the outside, the original crystal looks like a parallel aggregate. However, effectively, it can be considered as a single crystal (Fig. 22f).

In Figure 25b, the ratio of growth rates of tourmaline versus quartz was smaller. As a result and in contrast to the former examples, the outer surface of the aggregate is here dominated by quartz crystals and not by tourmaline. These observations led to a study of crosscuts of twenty other parallel aggregates from different locations (some examples are shown in Fig. 24).

The author expected to see a massive central "mother" crystal, on which the parallel second generation of daughter crystals had grown, a well-known phenomenon with quartz, calcite and fluorite, among other minerals (Rustemeyer 2018). Instead, all the crystals are dendritic, like the ones presented in Figs 22b, d and e, with arms growing from the edges of a central crystal. In Figs 22d and e, the overgrown tourmaline was graphically removed in the lower picture to make the fluffy array of dendrites more clearly visible.

Only some parallel aggregates, like those in Figs 22e and f, show a hollow central crystal. The longitudinal cut in Fig. 22f indicates that the central crystal is, in this case, hollow only in the central part of the tourmaline.

The author made a pertinent observation in this context of parallel aggregates in skeletal and dendritic crystals (Rustemeyer 2017, 2019a; Stroppini 2019). A few years ago, Angelo Stroppini, a Swiss collector, succeeded in finding and opening a pocket of about 1 m in diameter, an important find in the Misox Valley, Grison, Switzerland. The pocket contained many tourmaline crystals up to 25 cm in length. About one-third of them grew as compact single crystals, and two-thirds looked like parallel aggregates (the right-hand crystal in Fig. 24 is an example). The compact crystals have a classical blue core and rim; only the outer rim layer is brown. An example of a slice of the parallel aggregates is given in Fig. 22e. These crystals started to grow as a fluffy dendritic array in blue, later followed by a short interval of brown overgrowth. The same sequence of colors strongly suggests that both types of tourmaline grew simultaneously.

An interesting question arises: why did two morphologically differently tourmalines, one compact and the other dendritic, grow simultaneously in the same pocket? The phase-separation hypothesis (London 2013, 2016; Thomas
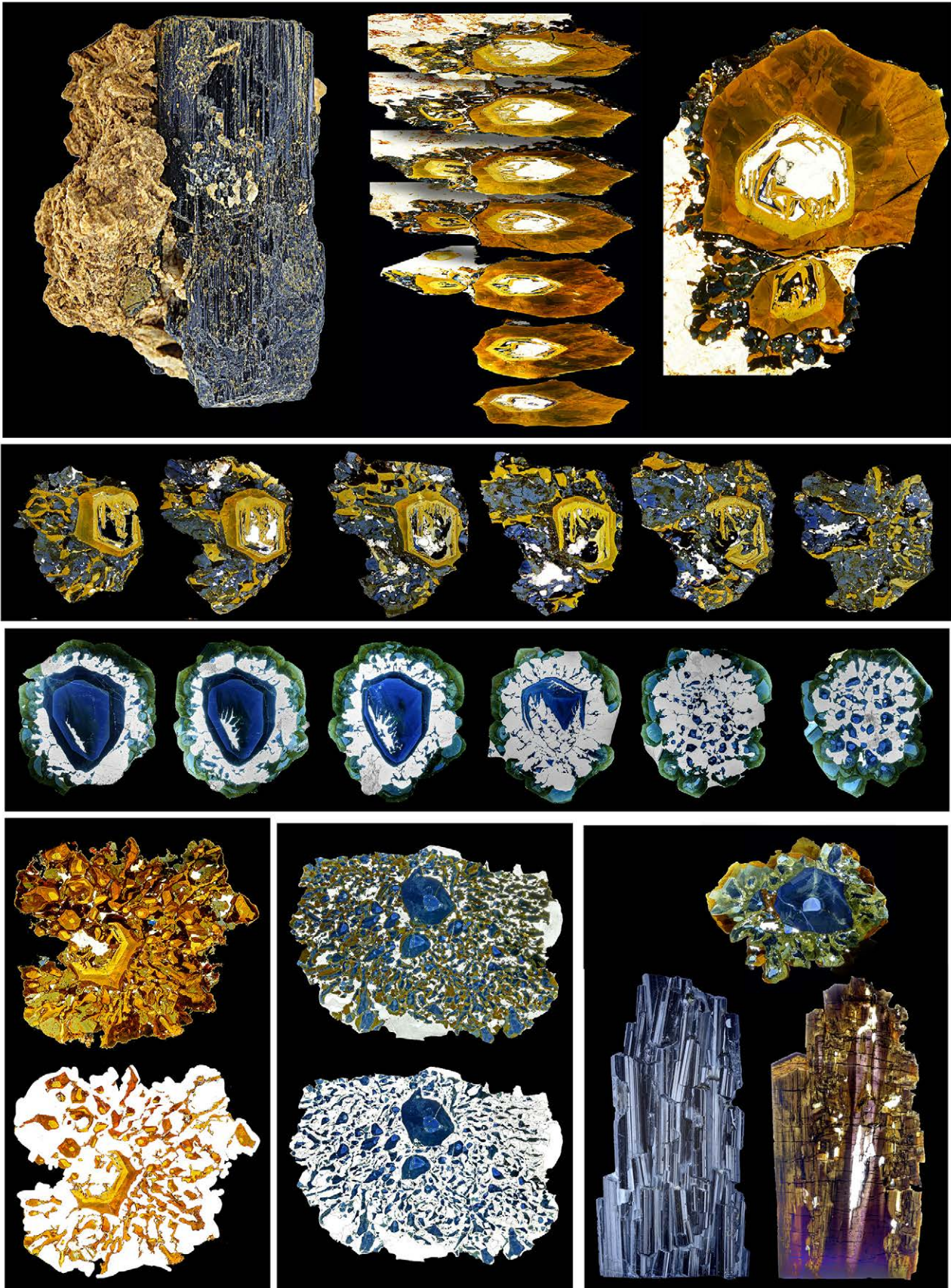
**Fig. 23** Skeletal and dendritic tourmaline in a longitudinal cut (7 cm wide) through a tubular crystal and crosscuts (5 cm wide) of varied thickness. Wolkenburg pegmatite, Penig, Saxony, Germany.

and Davidson 2016) could well explain this finding. When the water-rich melt cooled, bubbles of a supercritical aqueous fluid separated from the melt. Tourmalines may then grow simultaneously from the melt and from the aqueous fluid. Distinct morphologies are to be expected. In the aqueous bubbles, the mass transport of dissolved nutrients is easy, and compact crystals should grow. In the much more viscous melt, diffusion is limited and difficult; skeletal and dendrite formations are to be expected.

## 7.4. Parallel aggregates of tourmaline crystals grown on a dendritic intergrowth of tourmaline with quartz, feldspar or mica

In contrast to the preceding examples, there are also cases of dendritic crystals without skeletal hollow or compact

⇦

**Fig. 22** Skeletal and dendritic growth in tourmaline. **a** – A freely formed skeletal crystal of tourmaline. The yellowish tube in the center is the sector zone of the pyramidal faces. It widens toward the top. Apatite pocket, Amerika quarry, Penig, Saxony, Germany, Ø 1.2 cm. **b** – Toward the top, the tube of this skeletal brownish tourmaline is transformed into a bundle of dendritic arms. Later, it was overgrown with blue tourmaline. Apatite pocket, Amerika quarry, Penig, Saxony, Germany, Ø 1.2 cm. **c** – Series of slices of a dark tourmaline; a hollow skeletal crystal in the center transitions into a bundle of dendritic arms. Laterally, a three-dimensional network of dendritic arms is embedded in quartz and leads to an overgrowth of a ring of parallel satellite crystals. Skardu, Pakistan, Ø 4 cm. **d** – Hollow skeletal crystal with a lateral dendritic network and several parallel satellite crystals. Below, the later layer was removed to monitor the initial network. Apatite pocket, Amerika quarry, Penig, Saxony, Germany, Ø 2 cm. **e** – The same as d, Misox valley, Grisons, Switzerland, Ø 5 cm. **f** – Parallel aggregate that contains similar structures as in c–e, Skardu, Pakistan, Ø 3 cm.

tourmaline in the center. Their three-dimensional network is filled with quartz, mica or feldspar (or all three). They are overgrown with parallel massive crystals (Figs. 25c, e, f). If the tourmaline is cut and sliced in the longitudinal direction (as in the crystal from the Resplendor mine in Minas Gerais: Steger 2011; Fig. 25c), a typical pattern of more or less horizontal and vertical dendrite branches becomes visible. In the lower middle portion, the dendritic structure is quite fine, and it becomes progressively coarser outward until the larger crystals overgrew the "tourmaline outcrops" and embedded the tourmaline–quartz intergrowth. The progressively coarsening pattern can be seen as an indication of a decreasing supersaturation. Also, in this case, the whole tourmaline structure is a single crystal.

The second example in Fig. 25e, from Mount Isa in Queensland, Australia, shows the same features. In contrast to all the tourmaline crystals presented so far, it did not grow in a pegmatite but rather under metamorphic conditions in schist (Carr 2008). The center, in this case, is an intergrowth of dravite and mica.

Crosscuts and longitudinal cuts of ten parallel aggregates from the Erongo Mountains in Namibia all show a dendritic inner morphology (Rustemeyer 2018). An example with an intergrowth of tourmaline and feldspar from Erongo is shown in Fig. 25f.

## 7.5. Graphic intergrowth of tourmaline and quartz with skeletal and dendritic morphology

Graphic intergrowths of tourmaline and quartz are commonly found in pegmatite dykes as compact greyish or black intergrowths. They have been well described (e.g., Credner 1875; Brammall and Harwood 1925; Manning 1982; Dietrich 1985; Longfellow and Swanson 2011). Their architecture becomes visible if thin and ultrathin sections are prepared as crosscuts or in the longitudinal direction. Figure 26 shows examples from Rožná (Czech Republic), Grotta di Oggi (Elba, Italy, Rustemeyer 2015b), Wolkenburg and Amerika quarry (near Penig in Saxony, Germany, Rustemeyer 2011, 2015a) and Freiburg (Germany: a sample of "Weißer Fels", Rustemeyer 2019b). These images and Fig. 23 show that the intergrowths are embedded in feldspar. The feldspar seems to have crystallized first; the remaining volume of viscous silicate melt commonly contains only one crystal of tourmaline that nucleated and formed a dendritic network as a result of a high supersaturation and inefficient diffusion. Quartz grew simultaneously. Intermediate stages must have looked like the crystals in Fig. 25b. Thus it is not surprising that the arrays resemble the ones seen within the parallel aggregates (Figs 22, 25).

Figure 26a shows how the three-dimensional evolution of an intergrowth of tourmaline and quartz can be fol-
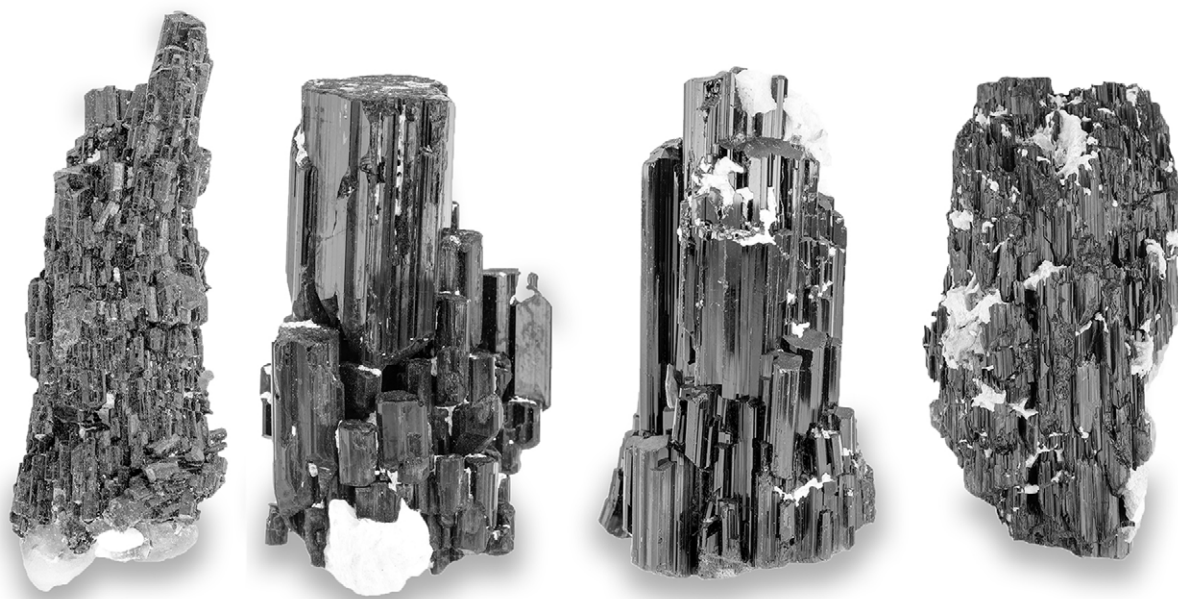
**Fig. 24** Parallel aggregates; from the left, Tokambohiorta, Sahatany valley (Madagascar), Shigar (Pakistan), Stak Nala, Gilgit (Pakistan), and Minas Gerais (Brazil), Ø 3–4 cm.

lowed through five consecutive slices. A central skeletal hollow tourmaline is transformed into dendritic arms, on which new compact tourmaline crystals nucleate. This evolution is comparable to that within the single crystals in Figs 22b and 22c. In many cases, the evolution of the graphic intergrowths of tourmaline and quartz takes place in parallel along several branches of the three-dimensional network.

The typical pattern of more or less horizontal and vertical branches of dendrite in the longitudinal cut in Fig. 26e is found again at the center of the parallel aggregates in Figs. 25c and 25e. A shell of parallel large single crystals grew on the dendritic intergrowth areas once oversaturation in quartz ended.

In larger graphic intergrowths of tourmaline and quartz, one can see here and there that the dendritic arms widen to build thicker crystals, which then transform again into dendritic arms, again growing thicker, and so on. The process seen with the freely grown crystals is repeated several times in the graphic intergrowth areas.

### 7.6. "Multicore" crystals grown on a graphic intergrowth

Figure 25f shows a simplified graphic example of dendritic tourmaline growth with frequent and simultaneous nucleation of quartz (Rustemeyer 2008, 2011). Eventually, quartz growth stops, and tourmaline continues to crystallize as free parallel crystals. The more they grow, the closer they come laterally. They then merge into a parallel aggregate on which, in the end, a common rim zone appears. Figure 25d shows an intermediate state with several parallel crystals of tourmaline, in some of which the roots are quite visible in the quartz–tourmaline intergrowth in the wall of the pocket.

Figure 27 shows a series of slices in which the lowermost contains about 15 parallel cores of tourmaline, an indication of derivation from a graphic intergrowth of tourmaline and quartz. Toward the top, these crystals merge and form one core zone. One sees that a single crystal of tourmaline can subdivide into a complex three-dimensional network and eventually reunify as one compact crystal.

## 8. Conclusions

New methods of making ultrathin sections showing an optimum depth of color have led to the detailed description of the morphological features and color zonation in numerous tourmaline crystals up to 10 cm in diameter. The various growth-induced morphological phenomena have led to complex three-dimensional architectures; several examples of the more commonly occurring phenomena include delta features (delta-shaped color domains), textural features associated with healing of corroded crystals, subdivision phenomena, and patterns of skeletal and dendritic growth in freely grown parallel aggregates as well as in graphically intergrown tourmaline and quartz. It seems likely more phenomena will be discovered with these refined methods. To date, this study has concentrated methodically on the morphology

**Fig. 25** Parallel aggregates of skeletal and dendritic crystals of tourmaline. **a** – A mostly skeletal central crystal is surrounded by dendritic arms overgrown with quartz. The "outcrops" of the tourmaline are overgrown with a ring of parallel satellite crystals. Series of slices from the Resplendor mine, Minas Gerais, Brazil, Ø 6 cm; the left slice is on top. **b** – The same structure as in **a** with a less dense ring of satellite crystals, from Grotta di Oggi, Elba, Italy, Ø 15 mm. **c** – Parallel aggregate of parallel crystals grown on the exposures of a monocrystalline dendrite that was intergrown with quartz, Minas Gerais, Brazil, 6 cm wide. **d** – Direct overgrowth of colored tourmaline on a dendritic intergrowth of quartz and tourmaline, 2 cm wide, collection of the Natural History Museum, Pisa. **e** – Same as in **c**, tourmaline dendrite is intergrown with mica, May Down Station, Mount Ida, Queensland, 6 cm wide. **f** – Aggregate of parallel crystals showing on the bottom a graphic intergrowth of tourmaline and feldspar, Erongo, Namibia, 7 cm wide.
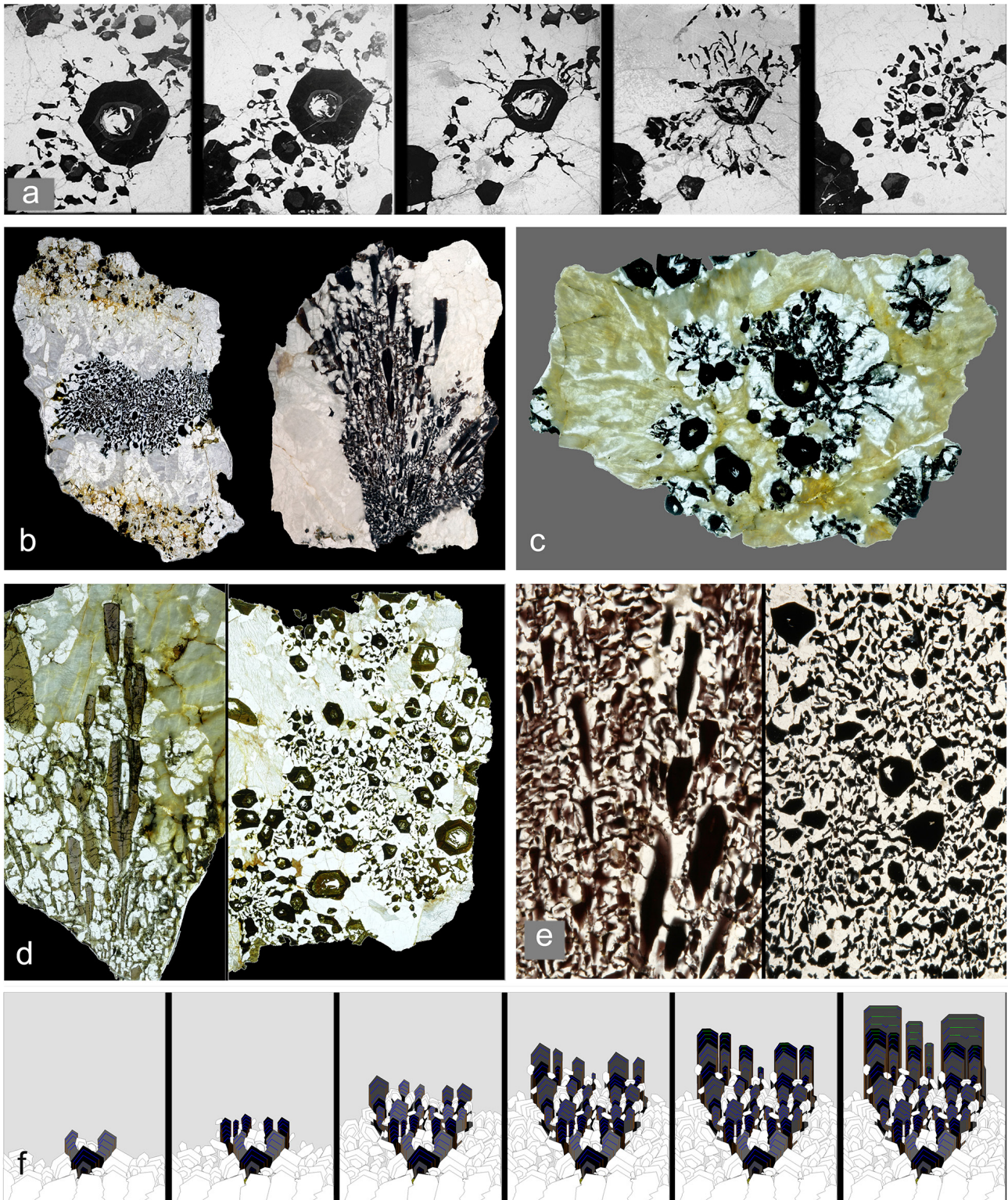
**Fig. 26** Graphic intergrowths of monocrystalline dendritic tourmaline and quartz.  **a** – Series of slices from a monocrystalline skeletal and dendritic crystal embedded in quartz, Rožná, Czech Republic 15 mm wide. The central skeletal crystal transitions into dendritic arms, as in Fig. 22b and 22c. **b** – Graphic intergrowth of monocrystalline dendritic tourmaline and quartz from Grotta di Oggi, Elba, in crosscut and longitudinal cut, 7 and 6 cm wide. **c** – Like **b**, from Wolkenburg, Penig, Saxony, Germany, 6 cm wide. **d** – Like **b,** longitudinal cut and crosscut from Weißer Fels, Freiburg, Germany, 5 cm wide (Rustemeyer 2019b). **e** – Like **b**, longitudinal cut and crosscut from Amerika quarry, Penig, Saxony, Germany. **f** – Simplified graphic experiment of dendritic tourmaline growth with frequent simultaneous quartz nucleation (Rustemeyer 2008, 2011).
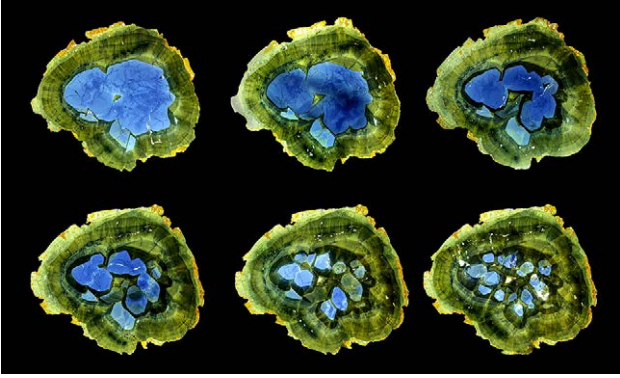
**Fig. 27** Series of slices with 14 parallel core zones in the lowest slice (bottom right), which unify toward the top of the crystal. Coronel Murta, Minas Gerais, Brazil, Ø 4 cm.

of color zones. More insight can be gained in the future if these empirical observations are combined with modern analytical methods to determine crystallographic, compositional and structural features.

# References

ALLÈGRE CJ, PROVOST A, JAUPART C (1981) Oscillatory zoning: a pathological case of crystal growth. Nature 294: 223–228

BENESCH F (1985) Der Turmalin. Urachhaus, Stuttgart, Germany, pp 1–379

BOUDREAUX AP (2014) Mineralogy and Geochemistry of the Erongo Granite and Interior Quartz–Tourmaline Orbicules and NYF-Type Miarolitic Pegmatites, Namibia. M.S. thesis, University of New Orleans, New Orleans, Louisiana, USA

BRAMMALL A, HARWOOD HF (1925) Tourmalinization in the Dartmoore Granite. Mineral Mag 20: 319–330

CARR PF (2008) Dravite from May Downs, Mount Isa, Queensland. Aust J Miner 14: 81–87.

CREDNER H (1875) Die granitischen Gänge des sächsischen Granulitgebirges. Z Dtsch geol Gesell 27: 104–223

DIETRICH RV (1985) The Tourmaline Group. Van Nostrand Reinhold, New York, N.Y., USA pp 1–287

DOWTY E (1976) Crystal structure and crystal growth: II. Sector Zoning in minerals. Amer Miner 61: 460–469

DUTROW BL, HENRY DJ (2000) Complexly zoned fibrous tourmaline: A record of evolving magmatic and hydrothermal fluids. Canad Mineral 38: 125–137

FALSTER AU, SIMMONS WB, WEBBER KL, BOUDREAUX AP (2018) Mineralogy and geochemistry of the Erongo subvolcanic granite – miarolitic pegmatite complex, Erongo, Namibia. Canad Mineral 56: 425–449

GOLDSCHMIDT V (1923) Atlas der Krystallformen, Tafeln. Band IX, Carl Winters Universitätsbuchhandlung, Heidelberg, pp 1–128

HENRY DJ, DUTROW B (1996) Petrologic Aspects of Metamorphic Tourmaline. Rev Mineral Geochem 33: 503–558

HENRY DJ, DUTROW BL, SELVERSTONE J (2003) Compositional asymmetry in replacement tourmaline—An example from the Tauern Window, Eastern Alps. Amer Miner 88: 1399–1399

HUMPHRIES DW (1992) The Preparation of Thin Sections of Rocks, Minerals, and Ceramics. Royal Microscopical Society Microscopical Handbooks no. 24, Oxford University Press, pp 1–83

KLEIN C, DUTROW BL (2007) Manual of Mineral Science. Wiley, pp 1–704

LACROIX A (1908) Les minéraux des filons de pegmatite à tourmaline lithique de Madagascar. Bull Minéral 31: 218–247

LONDON D (2013) Crystal-Filled Cavities in Granitic Pegmatites: Bursting the bubble. Rocks Miner 88: 527–534

LONDON D (2016) Reading pegmatites: what tourmaline says. Rocks Miner 91: 132–149

LONGFELLOW KM, SWANSON SE (2011) Skeletal tourmaline, undercooling, and crystallization history of the Stone Mountain granite, Georgia, U.S.A. Canad Mineral 49: 341–357

LUSSIER AJ, HAWTHORNE FC (2011) Oscillatory zoned liddicoatite from Anjanabonoina, central Madagascar. II. Compositional variation and mechanisms of substitution. Canad Mineral 49: 89–104

MANNING DAC (1982) Chemical and morphological variation in tourmalines from the Hub Kapong batholith of peninsular Thailand. Mineral Mag 45: 139–147

PEETSCH J (2011) Madasgaskar: Die Wiederentdeckung einer Turmalinmine. Extra Lapis Turmalin II: 62–65

RAKOVAN J (2009) Sectoral Zoning. Rocks Miner 84: 171–176

REED FS, MERGNER JL (1953) Preparation of rock thin sections. Amer Miner 38: 1184–1203

Rustemeyer P (2003a) Ungewöhnliche Turmaline vom Erongo, Namibia. Lapis 11: 29–41

Rustemeyer P (2003b) Faszination Turmalin. Spektrum Akademischer Verlag Weinheim, Germany, pp 1–308

Rustemeyer P (2008) Graphische Verwachsungen von Turmalin und Quarz. Lapis 33: 37–44

Rustemeyer P (2009) Quarz – Formen, Farben, Varietäten. Extra Lapis 37: 1–98

Rustemeyer P (2011) Turmalin II. Extra Lapis pp 1–102

Rustemeyer P (2014a) Der Erongo, Namibias produktivstes Fundgebiet der letzten zehn Jahre. Extra Lapis Namibia: 14–29.

Rustemeyer P (2014b) Die hohlen Turmalinkristalle aus der klassischen Fundstelle von Wolkenburg. Veröff.Mus f Naturk Chemnitz 37: 5–10

Rustemeyer P (2015a) Tourmaline – Fascinating Crystals with Fantastic Inner Worlds. Verlag Dr. Friedrich Pfeil, München, Germany, pp 272

Rustemeyer P (2015b) Turmaline aus Elba: Ihre Vielfalt und ihre Entstehung. Lapis 40: 30–40

Rustemeyer P (2017) Graubündner Turmalinschätze. Lapis 42: 10–17

Rustemeyer P (2018) Kristall Phänomene – Skelette, Dendriten und orientierte berwachsungen. Extra Lapis 54: 1–122

Rustemeyer P (2019a) Die Turmaline des Jahrhundertfundes aus dem südlichen Misox-Tal. Schweizer Strahler 53: 2–16

Rustemeyer P (2019b) Schwarzwälder Turmaline. Der Erzgräber 34: 1–76

Rustemeyer P (2022) Was die faszinierenden Strukturen im Innern dunkler Turmaline erzählen können. Der Aufschluss 73: 1–25

Rustemeyer P, Müller T (2017) Schwarze Turmaline aus Selb – mit farbigem Innenleben! Lapis 42: 24–31

Rustemeyer P, Prögler T (2019) Besondere Turmaline aus Herzogau und Althütte im Bayr. Wald Lapis 44: 24–31

Steger G (2011) Minen in Minas Gerais. Extra Lapis Brasilien 40: 64–68

Stroppini A (2019) Die Entdeckung einer großen Pegmatitgeode im Misox (GR). Schweizer Strahler 53: 2–14

Sunagawa I (2005) Crystals – Growth, Morphology and Perfection. Cambridge University Press, Cambridge, U.K, pp 1–308

Thomas R, Davidson P (2016) Revisiting complete miscibility between silicate melts and hydrous fluids, and the extreme enrichment of some elements in the supercritical state – Consequences for the formation of pegmatites and ore deposits. Ore Geol Rev 72: 1088–1101

Van Hinsberg VJ, Schumacher JC, Kearns S, Mason PRD, Franz G (2006) Hourglass sector zoning in metamorphic tourmaline and resultant major and trace-element fractionation. Amer Miner 91: 717–728